



PII S0016-7037(01)00677-9

The geochemical consequences of late-stage low-grade alteration of lower ocean crust at the SW Indian Ridge: Results from ODP Hole 735B (Leg 176)

WOLFGANG BACH,^{1,*} JEFFREY C. ALT,² YAOLING NIU,³ SUSAN E. HUMPHRIS,⁴ JÖRG ERZINGER⁵, and HENRY J. B. DICK⁴Departments of ¹Marine Chemistry and Geochemistry, ²Department of Geological Sciences, 2534 C.C. Little Building, University of Michigan, Ann Arbor, MI 48109-1063, USA³Department of Earth Sciences, University of Queensland, Brisbane, Queensland 4072, Australia⁴Geology and Geophysics, Woods Hole Oceanographic Institution, Woods Hole, MA 02543, USA⁵GeoForschungsZentrum Potsdam, Telegrafenberg Haus B, D-14473 Potsdam, Germany

(Received August 10, 2000; accepted in revised form May 10, 2001)

Abstract—Chemical exchange between oceanic lithosphere and seawater is important in setting the chemical composition of the oceans. In the past, budgets for chemical flux in the flanks of mid-ocean ridges have only considered exchange between basalt and seawater. Recent studies have shown that lower crustal and upper mantle lithologies make up a significant fraction of sea floor produced at the global mid-ocean ridge system. Moreover, the rugged topography of slow spread crust exposing lower crust and upper mantle facilitates prolonged fluid circulation, whereas volcanic ridge flanks are more rapidly isolated from the ocean by a sediment seal. Hence, elemental fluxes during lower crust–seawater reactions must be assessed to determine their role in global geochemical budgets.

ODP Hole 735B penetrates more than 1500 m into lower ocean crust that was generated at the very slow spreading Southwest Indian Ridge and later formed the 5-km-high Atlantis Bank on the inside corner high of the Atlantis II Fracture Zone. The gabbroic rocks recovered from Hole 735B preserve a complex record of plastic and brittle deformation and hydrothermal alteration. High-temperature alteration is rare below 600 m below seafloor (mbsf), but the lowermost section of the hole (500–1500 mbsf) has been affected by a complex and multistage low-temperature (<250°C) alteration history probably related to the tectonic uplift of the basement. This low-T alteration is localized and typically confined to fractured regions where intense alteration of the host rocks can be observed adjacent to veins/veinlets filled with smectite, smectite–chlorite mixed layer minerals, or chlorite ± calcite ± zeolite ± sulfide ± Fe-oxyhydroxide.

We have determined the bulk chemistry and O and Sr isotope compositions of fresh/altered rock pairs to estimate the chemical fluxes associated with low-temperature interaction between the uplifted and fractured gabbroic crust and circulating seawater. The locally abundant low-temperature alteration in crust at Site 735 has significantly changed the overall chemical composition of the basement. The direction of these changes is similar to that defined for volcanic ridge flanks, with low-temperature alteration of gabbroic crust acting as a sink for the alkalis, H₂O, C, U, P, ¹⁸O, and ⁸⁷Sr. The magnitudes of element fluxes are similar to volcanic ridge flanks for some components (C, P, Na) but are one or two orders of magnitude lower for others. The flux calculations suggest that low-temperature fluid circulation in gabbro massifs can result in S uptake (3% of riverine sulfate input) in contrast to the S losses deduced for volcanic ridge flanks. Copyright © 2001 Elsevier Science Ltd

1. INTRODUCTION

Circulation of seawater in ocean crust results in reactions between fluid and basement that have consequences for the chemical and isotopic composition of both the aging ocean crust and seawater. Focused discharge of high-temperature hydrothermal fluids at or near the axis of mid-ocean ridges (Campbell et al., 1988; Corliss et al., 1979; Von Damm et al., 1985) delivers base metals, H₂S, and other chemical species to the seafloor, resulting in the formation of sulfide deposits (Edmond et al., 1979; Haymon and Kastner, 1981; Koski et al., 1984; Tivey, 1995) and supporting microorganisms that represent the food source for the unique vent biota at active hydrothermal systems (Jannasch and Mottl, 1985).

However, in terms of transport of heat and many components (e.g., the alkalis, Ca, U, Mg, P, ⁸⁷Sr, ¹⁸O, C), seawater circu-

lation in ridge flanks plays an important role rivaling that of axial hydrothermal systems (Alt and Teagle, 1999; Alt et al., 1996; de Villiers and Nelson, 1999; Elderfield et al., 1999; Hart and Staudigel, 1982; Mottl and Wheat, 1994; Staudigel et al., 1989; Staudigel et al., 1996; Stein et al., 1995; Wheat and Mottl, 2000). Estimates of geochemical fluxes and the role of ridge flank circulation in global geochemical budgets have relied on determination of the magnitudes of chemical change in altered rocks from drill holes (Alt and Teagle, 1999; Alt et al., 1996; Hart and Staudigel, 1982; Staudigel et al., 1989), or on linking fluid data (pore waters and off-axis spring waters) with heat flow measurements (Mottl and Wheat, 1994; Sansone et al., 1998; Wheat and Mottl, 2000). Compositional data from drill holes indicate that basalt–seawater reactions in the upper 200 to 300 m of the crust have the largest effects on net fluxes of Li, K, Rb, Cs, U, B, ¹⁸O, ⁸⁷Sr, etc. into the crust, although there are considerable variations in the magnitude of elemental fluxes (Alt et al., 1996; Staudigel et al., 1996).

However, mid-ocean ridges with slow spreading rates (<40

*Author to whom correspondence should be addressed (wbach@whoi.edu).

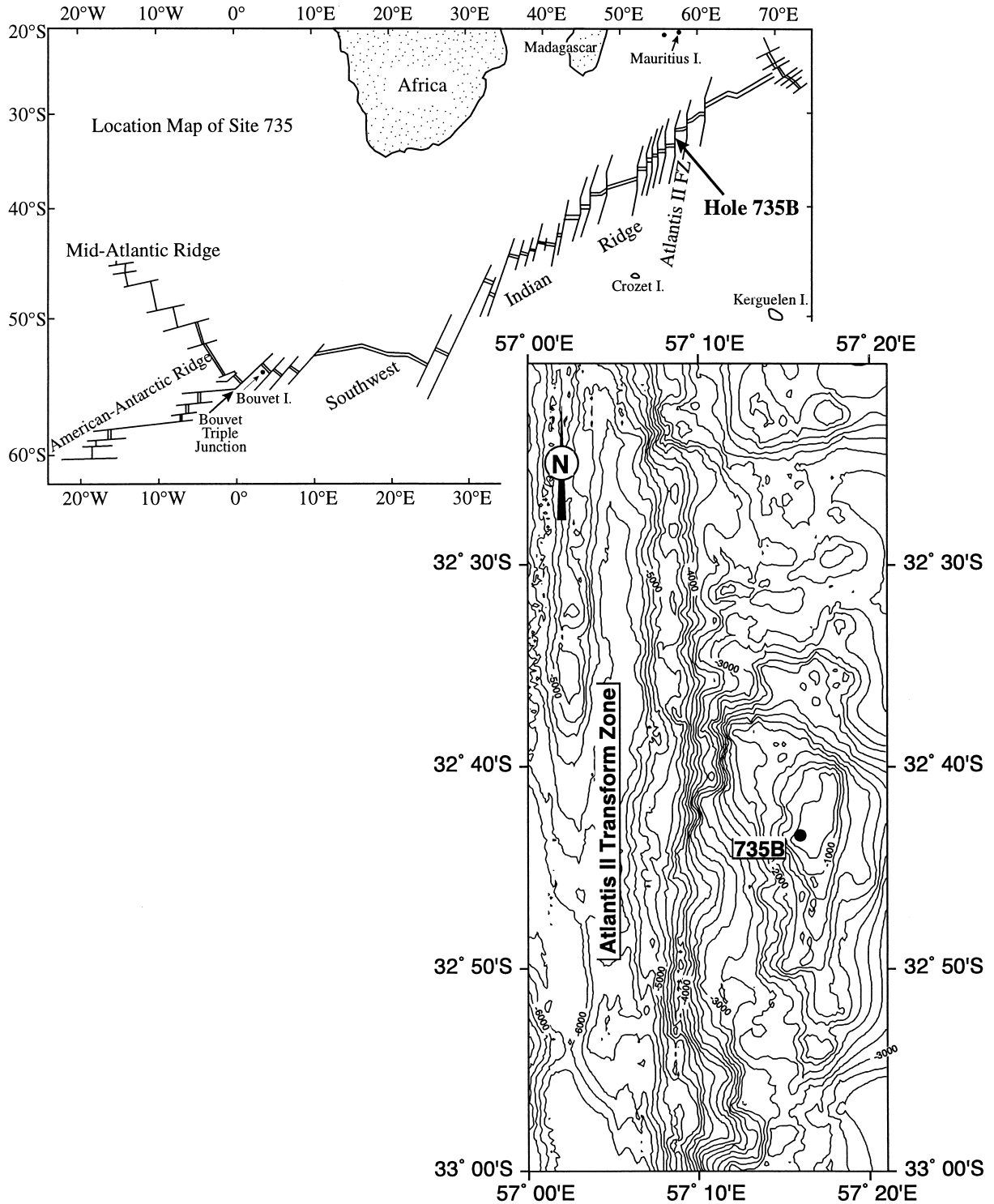


Fig. 1. Location map of ODP Site 735 east of the Atlantis II Fracture Zone on the Southwest Indian Ridge at 32°S, 58°E. Adapted from Dick et al. (1991b).

mm annual full spreading rate) are characterized by lithologically complex lithosphere that generally lacks a well-organized layer-cake structure (Cannat, 1996; Dick, 1989). The low magma budgets of slow spreading ridges lead to periods of

amagmatic extension and tectonic exhumation, during which lower crust and upper mantle are exposed to reaction with seawater (Cannat et al., 1997; Cannat et al., 1995; Tucholke and Lin, 1994; Tucholke et al., 1998). Given that slow spread-

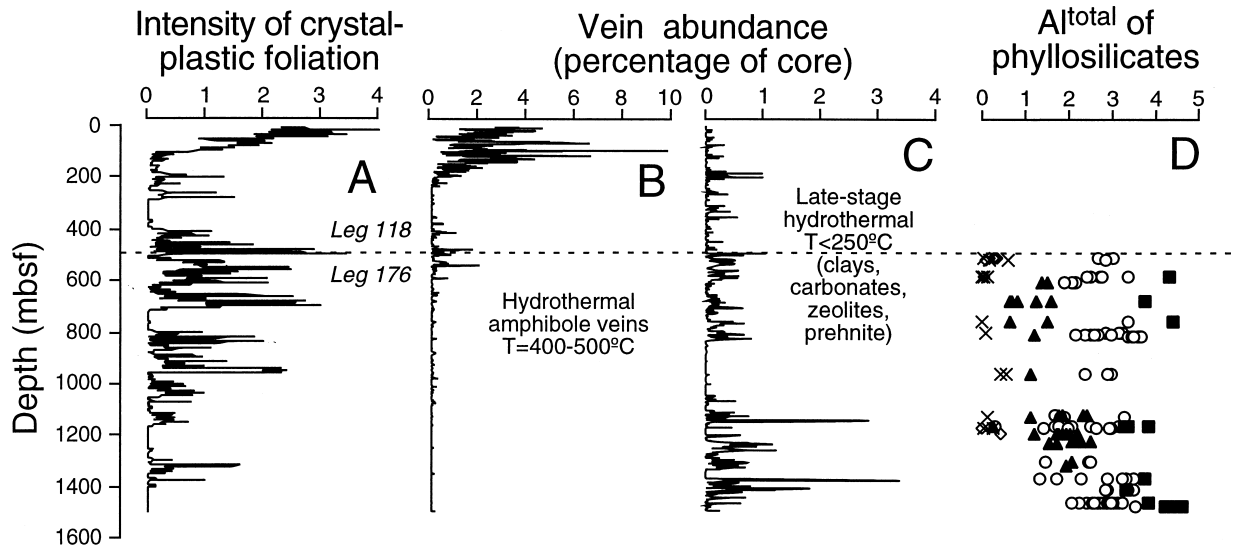


Fig. 2. Downhole variation of intensity of ductile deformation (A), abundances of amphibole veins (B), low-grade metamorphic veins (C), and Al^{total} values of phyllosilicates in veins and replacing olivine and pyroxene (D). Scale for intensity of crystal-plastic foliation varies from 0 (undeformed) to 5 (ultramylonite). Plotted trend is smoothed with a 2-m running window. Vein counts represent running averages for a 5-m window. See Shipboard Scientific Party (1999) for details. Al^{total} values are calculated based on $O = 28$. Different symbols are: squares, chlorite; circles, chlorite/smectite mixed-layer phases; triangles, smectite; X's, talc; and diamonds, serpentine [see Alt and Bach (2001) for details].

ing ridges constitute 52% by length of the global mid-ocean ridge system (Baker et al., 1996), lower crustal lithologies form a significant fraction of the flanks of slow spreading ridges. Hence, elemental fluxes during lower crust–seawater reactions must be assessed to determine their role in geochemical budgets.

This paper presents whole rock chemical and isotopic (Sr and O) data for “fresh”/“altered” sample pairs from the lower part of Ocean Drilling Program (ODP) Hole 735B at the Southwest Indian Ridge that was drilled during ODP Leg 176. Hole 735B has become a key section for lower ocean crust formed at very slow spreading ridges. We combine compositional data with estimated extents of low-grade background alteration (Shipboard Scientific Party, 1999) to derive the magnitude of chemical changes related to subgreenschist-facies alteration. We then compare the style and intensity of chemical alteration, together with flux estimates, to data for ridge flanks in layer-cake crust. Finally, we discuss the role that off-axis seawater circulation in slow and ultraslow spread crust might play in global seawater–lithosphere chemical exchange.

1.1. Hole 735B

Ocean Drilling Program (ODP) Hole 735B is located in the Atlantis II Transform Fault area at 57°E on the SW Indian Ridge (Fig. 1). It penetrates more than 1500 m into 12-my-old (John et al., 2001) gabbroic ocean crust that is exposed on a 5-km-high transverse ridge (Atlantis Bank) as a result of detachment faulting at the northern ridge–transform intersection of the SWIR from ~ 13 to 10 Ma (Dick et al., 1991b). Atlantis Bank now constitutes the eastern wall of the Atlantis II Fracture Zone. ODP Leg 118 recovered rocks to a depth of 500 mbsf; this was extended to 1508 mbsf on ODP Leg 176.

The gabbroic rocks recovered from Hole 735B preserve a complex record of magmatic, tectonic, and metamorphic processes (Dick et al., 2000; Von Herzen et al., 1989, 1999; Stakes et al., 1991; Vanko and Stakes, 1991). The metamorphic evolution starts with granulite-facies crystal-plastic deformation (at $T = 800\text{--}1000^\circ\text{C}$) in localized shear zones. A later alteration stage is indicated by coronitic alteration halos around olivine grains, and replacement of clinopyroxene and plagioclase by variable amounts of amphibole and chlorite. This so-called “static background alteration” is probably related to fluid ingress along cracks and microfractures. The alteration assemblages (talc, amphibole, magnetite, secondary clinopyroxene, chlorite, and smectite) reflect low water-to-rock ratios over a range of temperature from 600 to 700°C down to much lower temperatures. Subvertical amphibole veins formed at temperatures between 400 and 500°C and are probably related to cooling and cracking of the rocks in the axial environment (Stakes et al., 1991; Vanko and Stakes, 1991).

There is a general decrease in the intensity of deformation and hydrothermal alteration with increasing depth in Hole 735B (Fig. 2A, B). A close relationship between ductile deformation and fluid penetration is suggested by the correlation between amphibole contents and intensities of crystal plastic deformation, in particular in the uppermost 250 m (Cannat, 1991; Dick et al., 1991a; Dick et al., 2000; Stakes et al., 1991). Deeper in the hole, significant alteration is restricted to local zones of ductile and brittle deformation; i.e., in mylonitic and cataclastic shear zones or in highly fractured regions (Shipboard Scientific Party, 1999; Stakes et al., 1991). Below 700 mbsf, amphibole in veins and replacing magmatic minerals is rare, even in intensively deformed rocks (Fig. 2B), suggesting that fluid flow was minimal or temperatures were high and alteration is cryptic. However, local zones of high fracture

Table 1. Sample list with modal abundances of primary and secondary phases in thin section.

Sample	Core	Section	Top (cm)	Bottom (cm)	Piece	Depth (mbsf)	Primary mineralogy	OI	Plg	Cpx	Mt	Chl/Smct	Tlc	Carb	Hem	Sulf	Amph	Zeo	Others	% Altered
F1	91R	3	125	130	2	521.23	OG	22	58	10	2	4	1	1			2 ^a			8
A1-1	91R	3	100	105	1E	520.98	Fo78, An75		62	9	1	14	1	7	4		2 ^a			28
A1-2	91R	3	90	95	1D	520.88			58	10	1	10	1	14	4		2 ^a		Opx	30
F2	93R	1	75	81	5	532.88	DOxOG	3	57	32	2	3	1	1			1			6
A2	93R	1	86	91	5	532.99	Fo69, An51		50	36	1	9	Tr.	2	1		1			13
F3	102R	3	8	14	1	592.89	OxOG	2	66	25	1	5	1				Tr. ^a			6
A3	102R	3	1	8	1	592.83	Fo63, An49		55	36	1	6	Tr.	1	1		Tr. ^a			8
F4	103R	2	120	125	3F	597.42	OxOG	1	60	35	1	3	Tr.	Tr.			Tr.			3
A4	103R	2	139	142	4	597.60	Fo52, An53		45	41	1	9	1	1	1		1			13
F5	103R	4	36	45	4A	599.56	OG	3	48	41	1	3	2	Tr.			2 ^a			7
A5	103R	4	18	22	3	599.35	Fo67, An56		51	27	1	15	2	1	1		2 ^a			21
F6	127R	5	22	28	3	770.78	OG	2	65	27	1	5	Tr.				Tr.			5
A6	127R	5	12	20	2	770.69	Fo67, An56		63	22	1	13	Tr.	1			Tr.			14
F7	132R	1	94	99	11B	814.17	OG	2	44	44	2	8	Tr.	Tr.			Tr.			8
A7	132R	1	70	78	11A	813.94	Fo57, An55		50	28	1	18	Tr.	1			Tr.			21
F8	132R	8	112	118	7B	823.32	OG	6	43	46	1	4	Tr.	Tr.			Tr. ^a			4
A8	132R	8	103	109	7B	823.23	Fo58, An53		54	30	2	13	Tr.	Tr.			Tr. ^a			14
F9	150R	3	77	83	3	973.36	OG	11	43	43	1	2	Tr.				Tr.			2
A9	150R	3	65	69	2B	973.23	Fo67, An50		45	38	2	15	Tr.				Tr.			5
F10	168R	3	10	15	2	1133.02	OG	6	42	45	1	4	1				1			6
A10	168R	3	71	76	13	1133.63	Fo67, An54		57	27	2	12	1	Tr.			Tr.			15
F11	168R	7	36	41	3	1139.05	DOxOG	10	40	44	2	3	Tr.				Tr. ^a			3
A11	168R	7	7	13	2A	1138.75	Fo69, An54		52	36	2	10	Tr.	Tr.			Tr. ^a	Opx		10
F12	173R	4	94	100	4B	1183.61	DOxOG	6	48	39	1	5	Tr.				Tr.		Opx	6
A12-2	173R	4	115	119	5	1183.81	Fo69, An58		51	28	1	16	Tr.	1			Tr.	1 ^a		20
A12-1	173R	4	105	113	4B	1183.73			54	22	1	20	Tr.				Tr.	1		23
F13	177R	5	34	40	1A	1207.41	OG	11	50	35	1	3	Tr.				Tr.			3
A13	177R	5	50	56	2	1207.57	n.d.		44	25	1	29	Tr.	Tr.			Tr.			30
F14	180R	4	93	100	8	1235.75	OG	8	51	35	1	4	Tr.				Tr.			5
A14	180R	4	109	119	9C	1235.92	Fo72, An56		54	19	1	23	Tr.	Tr.			Tr.	2		26
F15	188R	7	61	68	1C	1316.00	OG	8	53	35	1	3	Tr.				Tr.			3
A15	188R	7	101	107	3A	1316.39	Fo73, An59		47	33	1	18					Tr.			19
F16	190R	2	69	75	1E	1327.95	OG	10	45	41	1	3					Tr.			3
A16	190R	2	97	103	2A	1328.23	Fo71, An53		53	30	1	14					Tr.			16
F17	207R	6	32	38	1	1476.27	OG	13	48	34	1	4					Tr.			4
A17	207R	6	32	38	1	1475.96	Fo75, An60		54 ^b	28	1	13					Tr.		Kfs	25
F18	209R	4	63	70	2B	1493.67	OG	11	49	25	1	12					Tr.			14
A18	209R	4	103	111	2B	1493.67	Fo75, An59		43	25	1	18					Tr.		Sphene	31

OG-olivine gabbro; DOxOG-disseminated oxide olivine gabbro; OxOG-oxide olivine gabbro; Ol-olivine; Plg-plagioclase; Cpx-pyroxene; Mt-magnetite; Chl/Smct-chlorite and chlorite/smectite mixed-layer phases; Tlc-talc; Carb-carbonate; FeOx-Fe-oxides and oxyhydroxides; Sulf-sulfides; Amph-amphibole; Zeo-zeolites, analcite, and prehnite; Opx-orthopyroxene; Kfs-potassium feldspar.

^a Includes trace amounts of magmatic hornblende.

^b 8% of the plagioclase is secondary albite.

Primary mineral analyses are reported in Dick et al. (submitted) and secondary mineral analyses are given in Alt and Bach (submitted).

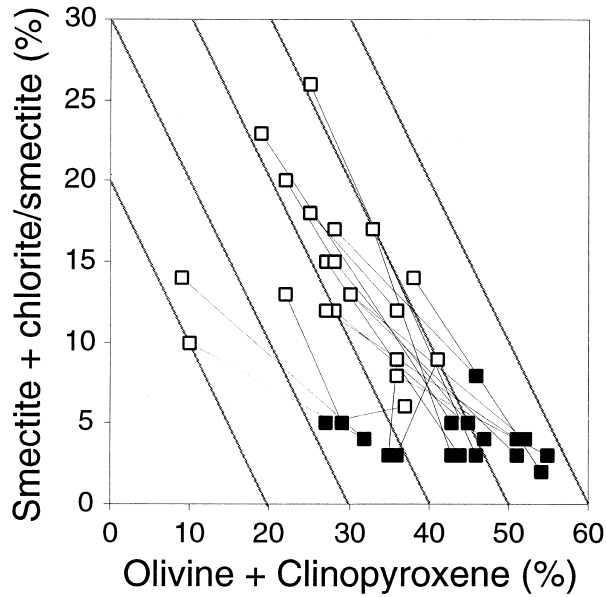


Fig. 3. Estimated modal abundances of low-grade smectite + chlorite/smectite mixed-layer phases versus modes for olivine + clinopyroxene. Filled symbols represent relatively fresh samples, and open symbols represent more altered samples. Tie lines connect fresh/alter sample pairs from the same section of drill core. Heavy lines indicate trends for isovolumetric replacement of olivine + clinopyroxene by smectite + chlorite/smectite mixed-layer phases. Note that for most samples replacement of mafic igneous minerals by low-grade phyllosilicates is the main alteration reaction. Samples with shallow sloping tie lines have significant amounts of calcite in addition to clay.

intensity and brittle deformation are commonly mineralized with low-temperature mineral assemblages (smectite, chlorite-smectite, carbonate, zeolites, analcite, and prehnite) even at great depths (Fig. 2C). In contrast to amphibolite-facies alteration, the distribution of these low-T alteration zones is not associated with plastic deformation. On the contrary, low-T vein intensity appears to be high (typically 15 veins/m) in zones with little or no crystal plastic foliation (Fig. 2, Shipboard Scientific Party, 1999). In contrast to the uppermost part of Hole 735B, low-temperature alteration is locally intense in the lower 1000 m, where high-temperature alteration is very weak.

In this paper, we focus on the geochemical consequences of low-grade alteration along late-stage brittle fractures in the lower section of 735B collected during ODP Leg 176. Low-temperature alteration is also present in the uppermost 500 m, but it is restricted to minor oxidative alteration at depths shallower than 40 mbsf (Hart et al., 1999) and to late-stage overprints in cataclastic zones that are impregnated with felsic magmatic veins and hydrothermal dioside-plagioclase veins (Stakes et al., 1991). Whereas the low-degree oxidative alteration is manifest as significant enrichments of Rb, Cs, and U, the geochemical effect of low-temperature alteration in the Leg 118 section is overall negligible compared to high-temperature hydrothermal and late-stage magmatic processes (Hart et al., 1999).

2. SAMPLES AND ANALYTICAL METHODS

A previous study (Hart et al., 1999) aimed at deriving a bulk composition of the uppermost 500 m of Hole 735B employed a strip-

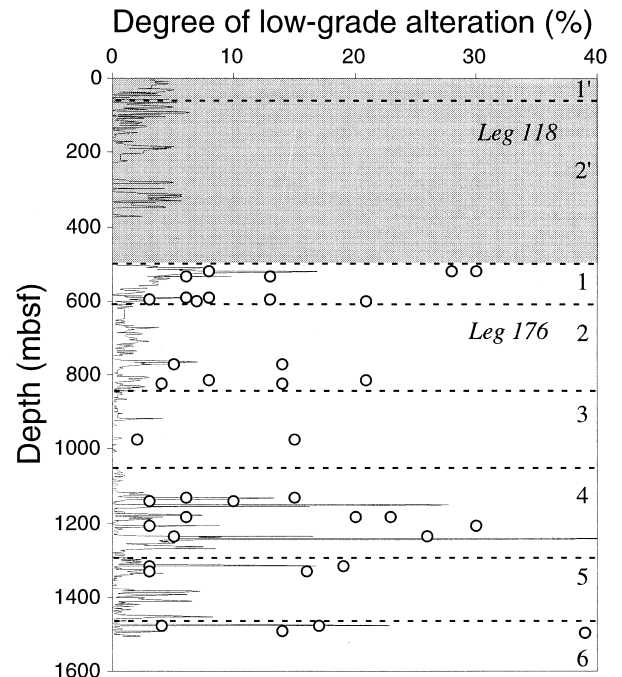


Fig. 4. Downhole log of low-grade background alteration (Bach and Humphris, unpublished data for depths < 500 mbsf; Shipboard Scientific Party, 1999 for depths > 500 mbsf). Open circles are the extents of alteration estimated from thin sections (Table 1). Discrepancies between the thin-section and visual core estimates are in part due to the fact that alteration is extremely heterogeneous and varies greatly on a cm scale. Horizontal dashed lines separate different alteration zones (cf. Table 2).

sampling technique to sample a long interval of core in a representative way. This sampling technique was not adopted for this study because we wished to examine chemical differences between fresh and altered rocks. Instead, 18 sets of fresh and altered rock samples were taken, with each set being selected from the same core section and the same igneous unit to minimize the possibility that observed chemical differences are primary features. Samples were characterized as "fresh" and "altered" based on the degree of low-grade alteration apparent in hand specimen. Coarse-grained samples and samples with felsic and oxide-rich impregnations were avoided because such lithologies are difficult to sample in a representative way given the relatively small sample volumes (typically 15 cm³). Major and trace elements were determined by inductively coupled plasma-optical emission spectroscopy (ICP-AES; Queensland University of Technology) and inductively coupled plasma mass spectrometry (ICP-MS; University of Queensland), following procedures outlined in Kwiecien (1990) and Niu and Batiza (1997). Ferrous iron was determined by manganometric titration, CO₂ and H₂O by a LECO analyzer RC-412, and sulfur analyses were carried out using a LECO sulfur determinator CS 225 (all at GFZ Potsdam). CO₂ data represent total carbon (carbonate, C, CH₄, and other reduced carbon species). Oxygen was extracted from whole-rock powders by reaction with ClF₃ and converted to CO₂ gas for measurement of oxygen isotope ratios at the University of Michigan. Repeated extractions and measurements of samples and standards were reproducible within $\pm 0.2\%$. Sr isotope analyses were carried out at Woods Hole Oceanographic Institution (WHOI), using a VG 54 thermal ionization mass spectrometer. Samples were dissolved with HF/HClO₄ in a Teflon beaker. Sr was separated on quartz columns with a 5-mL resin bed of AG50W-X12 200 to 400 mesh. ⁸⁷Sr/⁸⁶Sr ratios are reported relative to NBS 987 = 0.71024. External precision (2 σ) of Sr isotope analyses is 0.003%.

Table 2. Summary of low-grade secondary mineralogy and chemical effects of alteration in Hole 735B.

Zone	Depth range	Alteration phases	Alteration type, % altered ^a	Compositional changes
1'	0–40 mbsf	FeOx, Cc, Smct	Oxidative/3%	+Cs, Rb, K, U, P
2'	40–500 mbsf	Smct, Cc	Nonoxidative/2%	?
1	500–600 mbsf	FeOx, Cc, Non, Smct	Oxidative/8%	+U, CO ₂ , P, Cs, Rb, K, H ₂ O, ¹⁸ O, ⁸⁷ Sr –Si, Mg, Ca
2	600–835 mbsf	Chl/Smct, Smct, Cc, Pyr	Nonoxidative/2%	+CO ₂ , H ₂ O, ¹⁸ O, S, –Si
3	835–1050 mbsf	Chl/Smct, Smct, Cc, Pyr	Nonoxidative/<1%	Insignificant
4	1050–1300 mbsf	Chl/Smct, Smct, Analc	Nonoxidative/4%	+Li, K, Rb, Cs, ¹⁸ O, ⁸⁷ Sr, Na, S, CO ₂ , –Mg
5	1300–1475 mbsf	Chl/Smct, Zeo, Preh	Nonoxidative/2%	+CO ₂ , H ₂ O, ¹⁸ O, Na, –Mg
6	1475–1506 mbsf	Chl, Chl/Smct, Act, Ab	Greenschist-fac./2%	+ ¹⁶ O, Si, Na, –Mg

FeOx = Fe-oxyhydroxides; Cc = calcite; Non = nontronite; Smct = smectite; Chl/Smct = chlorite/smectite mixed-layer phases; Pyr = pyrite; Analc = analcite; Zeo = zeolites; Preh = prehnite; Chl = chlorite; Act = actinolite; Ab = albite; “+” = gain, “–” = loss.

Mineralogy and chemistry of low-temperature overprint within upper 500 mbsf are from Stakes et al. (1991) and Hart et al. (1999).

^a % altered is the estimated percentage of low-grade alteration in the drill core (cf. Fig. 4).

3. RESULTS AND DISCUSSION

3.1. Modal Mineralogy and Mineral Replacement

Visual thin-section estimates of primary and secondary modes and the degree of alteration (percentage of secondary minerals) are reported in Table 1. Even the samples characterized as “fresh” are slightly altered. Most of the fresh and altered rocks show evidence for small extents of high-temperature static background alteration (cf. Section 1.1) that is manifest as replacement of olivine and plagioclase by chlorite, amphibole, and talc (Table 1). Such low degrees of high-T alteration have been shown to have minimal chemical consequences for bulk rock chemistry of rocks with basaltic composition (Bach et al., 1996; Fletcher et al., 1997).

Superimposed on the high-temperature static background alteration are different styles of low-grade alteration that are most likely related to fluid percolation during the uplift and fracturing of the basement block to form the transverse ridge and core complex. Only the chemical consequences of this low-grade alteration are the subject of this paper. Late-stage circulation of seawater resulted in locally intense alteration of gabbros under subgreenschist facies conditions. Phyllosilicate mineralogy and isotope compositions reflect alteration under varying temperatures (<100–300°C) and fluid compositions (Alt and Bach, 2001). By volume, replacement of mafic minerals by phyllosilicates is the most important replacement reaction. This is demonstrated in Figure 3, where the tie lines between most fresh/alterated sample pairs plot parallel to lines for isovolumetric replacement of olivine and pyroxene by smectite and chlorite/smectite mixed-layer phases. Tie lines with shallower slopes indicate significant fractions of calcite or zeolites in addition to phyllosilicates.

The intensity of low-grade alteration is highly variable, as depicted in Figure 4. Based on variation in alteration intensity, visual core inspection of style, and intensity of low-grade alteration (Shipboard Scientific Party, 1999), as well as secondary mineralogy (thin-section petrography and electron microprobe work; Alt and Bach, 2001), six different alteration zones have been distinguished below 500 mbsf (Table 2):

(1) A zone from 500 to 600 mbsf is characterized by intense fracturing in the vicinity of brittle faults, with formation of carbonate, saponite, nontronite, celadonite layers in smec-

tites, and Fe-oxyhydroxides in veins and replacing olivine and plagioclase in vein halos. The lowermost samples from Leg 118 do not show the same style of alteration, so that this zone does indeed begin at a depth of 500 mbsf. Nontronite, the presence of celadonite layers in clays, and the abundance of Fe-oxyhydroxide indicate reaction of the rocks with oxygen-rich fluids, probably fairly unreacted seawater. O isotope compositions of the carbonates suggest very low formation temperatures of around 10°C (Alt and Bach, 2001), similar to the present-day temperature for the upper 500 m of the hole (8.5°C; Shipboard Scientific Party, 1999). The presence of open fissures suggests that this zone has an increased permeability and may still be hydrologically active. The alteration style of gabbros in vein halos is similar to seafloor weathering, with replacement of olivine by “iddingsite,” a mixture of fine-grained clays, carbonates, oxides, and oxyhydroxides.

- (2) Between 600 and 835 mbsf, smectite and chlorite/smectite mixed-layer phases ± carbonate veins are still abundant locally, but Fe oxyhydroxides and nontronite are lacking, suggesting that alteration was nonoxidative. Reducing conditions are also indicated by secondary sulfides replacing olivine along with chlorite/smectite mixed-layer phases.
- (3) Alteration style between 835 and 1050 mbsf is similar to zone 2, but the extent of alteration is generally very weak.
- (4) From 1050 to 1300 mbsf, alteration is similar to the zone from 600 to 835 mbsf, but analcite is an additional secondary phase, replacing plagioclase and filling fractures.
- (5) Below 1300 mbsf, prehnite, analcite, zeolites, and local K-feldspar are frequently observed, whereas smectite disappears (Fig. 2C). The presence of prehnite and the lack of smectite below 1300 mbsf suggest slightly higher alteration temperatures below this depth. Increasing alteration temperatures can also explain the subtle increase in Al content of smectite (Fig. 2D).
- (6) Rocks below 1475 mbsf exhibit abundant greenschist-facies minerals (albite, chlorite, and actinolite), consistent with higher-temperature (>250°C) alteration (still low-grade) at depth.

Geochemical and mineralogical studies of rocks from Leg 118 (Stakes et al., 1991; Hart et al., 1999) have been used in combination with our own visual core descriptions to divide the

Table 3. Chemical and isotopic data of fresh and altered gabbros.

Sample depth	F1	A1-1	A1-2	F2	A2	F3	A3	F4	A4	F5	A5	F6	A6	F7	A7	F8	A8	F9	A9
<i>Major element concentration (wt. %)</i>																			
SiO ₂	46.37	42.31	38.16	51.67	50.19	50.98	51.43	53.10	49.79	51.26	50.39	51.20	50.68	49.12	47.56	50.84	49.72	50.80	49.86
TiO ₂	0.24	0.22	0.20	0.42	0.46	0.37	0.54	0.66	0.59	0.49	0.36	0.41	0.35	0.56	0.47	0.62	0.54	0.39	0.40
Al ₂ O ₃	20.32	22.20	20.57	18.08	15.65	20.88	14.02	21.18	13.76	15.65	17.42	20.66	19.97	14.46	15.79	15.18	17.14	14.88	15.10
FeO	5.07	1.20	0.86	3.25	3.76	2.66	3.93	3.06	4.11	4.94	3.59	2.95	2.81	4.69	6.17	6.57	3.69	6.57	4.82
Fe ₂ O ₃	1.62	4.61	4.50	1.68	2.69	1.88	1.60	0.42	2.78	0.58	1.89	1.15	1.45	2.07	0.56	0.94	2.45	1.23	2.33
MnO	0.11	0.09	0.08	0.11	0.14	0.08	0.14	0.08	0.16	0.12	0.11	0.08	0.10	0.15	0.14	0.16	0.13	0.16	0.15
MgO	11.77	4.22	3.55	6.97	7.85	4.98	9.16	4.21	8.97	9.45	8.45	5.78	6.69	9.66	9.97	9.33	8.21	10.16	9.75
CaO	11.15	15.67	20.26	13.25	14.14	12.77	15.87	12.01	14.91	14.01	12.31	13.43	13.77	14.40	12.32	12.87	12.83	12.13	12.87
Na ₂ O	2.38	2.82	2.46	3.55	3.10	3.45	2.39	4.08	2.52	2.68	3.16	3.53	3.28	2.52	2.70	2.83	3.17	2.73	2.67
K ₂ O	0.05	0.20	0.09	0.06	0.07	0.08	0.08	0.10	0.09	0.13	0.10	0.06	0.05	0.05	0.05	0.04	0.05	0.04	0.04
P ₂ O ₅	0.01	0.10	0.20	0.01	0.05	0.04	0.02	0.05	0.01	0.02	0.05	0.04	0.02	0.05	0.03	0.04	0.06	0.03	0.01
H ₂ O	1.03	2.45	1.81	0.77	1.32	0.84	0.76	0.49	1.28	0.90	1.97	0.81	1.08	1.52	2.29	0.57	1.70	0.42	1.63
CO ₂	0.30	3.96	8.10	0.33	1.08	0.16	0.35	0.09	0.45	0.11	0.74	0.10	0.35	0.15	0.60	0.08	0.15	0.06	0.11
S	0.03	0.02	0.03	0.01	0.02	0.01	0.01	0.04	0.01	0.03	0.03	0.01	0.02	0.18	1.18	0.10	0.24	0.07	0.06
Total	100.45	100.07	100.87	100.14	100.52	99.18	100.28	99.57	99.44	100.37	100.57	100.21	100.60	99.58	99.84	100.18	100.07	99.67	99.81
L.O.I.	0.98	6.19	9.40	1.07	1.60	0.91	0.95	0.41	1.51	0.77	2.62	0.77	1.27	1.35	2.90	0.14	1.68	0.06	1.73
FeO ^{total}	6.53	5.35	4.91	4.76	6.18	4.36	5.37	3.44	6.62	5.47	5.29	3.98	4.11	6.56	6.67	7.42	5.89	7.68	6.92
Mg#	78.12	60.96	58.90	74.37	71.55	69.36	77.16	70.80	72.87	77.40	75.98	74.19	76.30	74.48	74.74	71.36	73.38	72.39	73.62
Fe ³⁺ /Fe ^{total}	0.224	0.776	0.825	0.317	0.392	0.389	0.268	0.110	0.379	0.096	0.322	0.259	0.317	0.285	0.076	0.114	0.374	0.144	0.303
<i>Trace element concentration (ppm)</i>																			
Li	3.56	5.41	2.95	3.54	2.44	8.35	7.50	2.74	11.76	4.69	7.32	3.38	4.58	4.66	6.28	3.18	4.14	2.46	4.88
Be	0.15	0.18	0.14	0.25	0.23	0.16	0.13	0.45	0.19	0.12	0.21	0.18	0.12	0.22	0.29	0.20	0.24	0.10	0.09
Sc	9.7	14.4	8.8	34.3	45.5	25.9	57.7	26.4	58.2	53.3	33.3	30.3	32.2	56.0	39.2	44.2	42.6	38.6	48.4
V	48	64	60	127	173	107	213	109	225	168	124	118	122	200	151	169	162	157	170
Cr	67	66	82	37	53	86	209	69	128	130	88	80	87	232	191	51	63	24	29
Co	50.2	42.2	41.5	30.7	36.8	37.2	48.1	18.0	34.0	34.5	32.3	24.8	27.2	35.3	37.0	42.6	37.7	55.0	48.5
Ni	309.2	184.5	167.3	52.5	69.7	70.4	86.9	45.7	74.3	68.8	62.7	54.9	61.5	67.2	70.9	64.2	70.2	75.4	70.7
Cu	49.9	48.3	37.8	30.6	41.1	57.5	68.3	52.0	66.3	37.1	55.8	17.9	30.3	58.7	70.9	55.9	36.8	68.2	69.1
Zn	35.5	31.5	29.4	24.8	32.4	38.2	49.4	25.3	42.7	32.7	29.0	21.6	22.3	37.1	33.4	44.9	34.1	39.2	33.6
Ga	11.5	12.5	11.7	14.1	13.1	14.6	11.3	17.1	12.0	11.6	12.5	15.0	14.2	11.8	12.3	12.9	13.7	13.0	12.9
Rb	0.20	3.23	0.72	0.31	0.41	0.90	0.77	0.27	0.39	0.80	0.41	0.30	0.22	0.26	0.24	0.13	0.23	0.07	0.15
Sr	166.5	196.0	237.9	193.3	154.4	209.7	136.1	217.0	136.0	151.3	159.2	198.4	185.3	127.9	139.6	155.3	156.0	160.1	150.3
Y	165.2	193.4	233.1	191.3	151.8	205.1	133.3	133.3	131.3	147.3	156.2	191.9	180.2	123.3	134.8	151.1	152.5	153.4	143.8
Zr	4.1	4.9	3.8	14.5	16.1	9.2	14.9	13.6	16.9	11.2	10.2	9.3	8.0	18.0	13.7	15.0	11.8	9.1	9.6
Nb	7.7	7.3	6.2	40.9	34.5	20.4	20.1	26.4	26.2	18.4	15.5	17.6	11.7	30.8	40.9	33.1	28.1	11.6	9.5
Cs	0.093	0.124	0.100	0.564	0.269	0.295	0.191	1.080	0.236	0.243	0.221	0.282	0.144	0.294	0.514	0.389	0.384	0.102	0.058
Ba	0.008	0.268	0.051	0.010	0.019	0.042	0.015	0.034	0.012	0.008	0.005	0.024	0.001	0.006	0.001	0.001	0.001	0.001	0.003
Ba	2.50	4.78	4.07	5.86	3.49	3.27	3.03	5.89	3.68	4.48	3.35	3.54	2.99	2.96	2.58	2.99	2.79	2.18	2.08
Ba	2.39	4.85	4.07	6.00	3.51	3.83	3.37	3.37	3.80	5.63	3.50	4.14	4.26	2.85	2.76	2.97	2.87	2.63	12.08
La	0.52	0.71	0.56	1.70	1.21	0.86	0.74	2.27	0.95	0.72	0.96	0.98	0.57	1.08	1.51	1.11	0.97	0.45	0.38
Ce	1.55	1.86	1.39	5.37	4.27	2.72	2.73	6.51	3.28	2.42	2.93	2.65	1.78	3.97	4.82	3.88	3.17	1.67	1.45
Pr	0.27	0.33	0.25	0.96	0.84	0.50	0.58	1.05	0.68	0.47	0.52	0.48	0.34	0.80	0.86	0.75	0.59	0.34	0.32
Nd	1.45	1.70	1.31	4.99	4.65	2.69	3.50	4.99	4.11	2.77	2.79	2.60	1.93	4.68	4.37	4.25	3.28	2.08	1.98
Sm	0.49	0.54	0.43	1.69	1.69	0.98	1.48	1.59	1.74	1.10	1.05	0.97	0.75	1.89	1.53	1.62	1.24	0.91	0.92
Eu	0.45	0.48	0.44	0.68	0.80	0.63	0.68	0.90	0.82	0.61	0.64	0.64	0.57	0.83	0.67	0.80	0.67	0.57	0.60
Tb	0.11	0.13	0.10	0.39	0.44	0.24	0.40	0.36	0.45	0.30	0.27	0.25	0.21	0.50	0.37	0.41	0.32	0.25	0.26

(Continued)

Table 3. (Continued)

Sample depth	F1	A1-1	A1-2	F2	A2	F3	A3	F4	A4	F5	A5	F6	A6	F7	A7	F8	A8	F9	A9
Gd	0.67	0.74	0.59	2.29	2.49	1.39	2.23	2.03	2.55	1.70	1.51	1.43	1.18	2.78	2.11	2.33	1.82	1.36	1.41
Dy	0.76	0.85	0.66	2.64	3.02	1.67	2.75	2.47	3.16	2.10	1.85	1.72	1.46	3.45	2.54	2.83	2.22	1.72	1.81
Ho	0.16	0.19	0.14	0.56	0.65	0.35	0.58	0.53	0.67	0.45	0.39	0.37	0.31	0.73	0.54	0.60	0.47	0.37	0.39
Er	0.45	0.53	0.40	1.57	1.79	1.00	1.62	1.51	1.86	1.23	1.11	1.03	0.86	2.04	1.54	1.69	1.31	1.02	1.08
Tm	0.07	0.08	0.06	0.23	0.27	0.15	0.24	0.23	0.27	0.18	0.17	0.15	0.13	0.31	0.23	0.26	0.20	0.15	0.16
Yb	0.44	0.51	0.38	1.45	1.65	0.90	1.44	1.42	1.69	1.12	1.05	0.94	0.77	1.87	1.40	1.55	1.21	0.94	0.98
Lu	0.07	0.08	0.06	0.22	0.24	0.14	0.21	0.22	0.25	0.16	0.16	0.14	0.11	0.28	0.21	0.24	0.18	0.14	0.15
Hf	0.253	0.258	0.199	1.104	1.023	0.603	0.714	0.880	0.876	0.633	0.538	0.536	0.375	1.023	1.102	0.988	0.803	0.419	0.393
Ta	0.010	0.011	0.015	1.563	0.033	0.047	0.017	0.083	0.417	0.023	0.022	0.025	0.013	0.028	0.039	0.032	0.041	0.022	0.007
Pb	0.218	0.400	0.310	0.348	0.308	0.310	0.352	0.613	0.312	0.587	0.369	0.224	0.193	0.558	1.348	0.299	0.892	0.159	0.185
Th	0.008	0.012	0.007	0.042	0.022	0.022	0.017	0.085	0.019	0.020	0.040	0.022	0.010	0.030	0.046	0.023	0.035	0.006	0.005
U	0.038	0.433	0.385	0.029	0.244	0.166	0.103	0.034	0.226	0.014	0.218	0.014	0.015	0.010	0.019	0.009	0.014	0.002	0.002
$\delta^{18}\text{O}$	6.77		8.15					6.5	6.02							5.97	6.58	5.99	6.05
$^{87}\text{Sr}/^{86}\text{Sr}$	0.703011	0.703766	0.704808	0.702989	0.703372	0.702865	0.703005	0.702833	0.702956	0.702861	0.702968	0.702790	0.702844	0.702842	0.702848	0.702822	0.702811	0.702799	0.702
Sample depth	F10	A10	F11	A11	F12	A12-1	A12-2	F13	A13	F14	A14	F15	A15	F16	A16	F17	A17	F18	A18
SiO ₂	50.84	51.89	49.18	51.00	49.66	49.79	49.88	48.72	48.56	50.76	49.44	51.04	49.88	50.24	50.67	49.79	50.29	48.20	48.89
TiO ₂	0.41	0.24	0.44	0.42	0.81	0.56	0.46	0.27	0.36	0.41	0.37	0.28	0.28	0.46	0.39	0.45	0.34	0.26	0.26
Al ₂ O ₃	15.19	21.50	14.15	17.59	16.31	18.42	16.92	16.70	15.36	15.92	17.79	16.45	15.03	14.46	16.72	11.82	18.32	16.50	14.79
FeO	n.d.	2.12	6.54	3.08	5.21	n.d.	1.99	5.64	3.79	4.79	3.21	4.32	3.78	5.22	3.60	5.59	3.24	4.95	5.19
Fe ₂ O ₃	n.d.	1.61	1.17	1.44	1.75	n.d.	1.99	1.00	2.59	1.15	2.23	0.99	2.46	1.41	2.04	1.33	1.57	1.37	1.09
MnO	0.13	0.07	0.16	0.11	0.14	0.09	0.11	0.12	0.12	0.12	0.10	0.11	0.12	0.14	0.11	0.15	0.10	0.11	0.11
MgO	10.09	5.18	11.64	7.38	9.33	6.72	7.80	11.03	9.87	10.18	8.58	9.85	10.62	11.25	7.81	14.57	8.22	11.68	11.59
CaO	13.79	11.77	13.10	14.23	12.92	11.76	13.43	11.90	11.92	12.95	11.16	13.17	12.91	13.36	12.20	14.40	13.45	11.76	12.18
Na ₂ O	2.55	3.69	2.45	3.06	2.75	4.00	3.17	2.70	3.15	2.69	3.28	2.60	2.39	2.69	3.16	1.75	2.87	2.39	2.47
K ₂ O	0.04	0.22	0.03	0.04	0.04	0.22	0.18	0.02	0.02	0.03	0.10	0.01	0.03	0.04	0.04	0.00	0.08	0.03	0.08
P ₂ O ₅	0.03	0.02	0.02	0.00	0.02	0.03	0.03	0.02	0.00	0.02	0.04	0.00	0.00	0.00	0.01	0.00	0.00	0.03	0.00
H ₂ O	0.71	1.62	0.50	0.89	0.85	2.82	2.29	0.57	3.61	0.82	3.43	0.52	2.40	0.51	2.09	0.61	1.36	1.78	2.58
CO ₂	0.08	0.28	0.09	0.11	0.08	0.23	0.76	0.08	0.19	0.08	0.18	0.09	0.23	0.09	0.16	0.10	0.16	0.07	0.13
S	0.06	0.08	0.07	0.04	0.08	0.45	0.17	0.04	0.24	0.13	0.15	0.06	0.15	0.06	0.29	0.04	0.15	0.06	0.05
Total	100.59	100.29	99.55	99.39	99.95	99.88	100.17	98.81	99.78	100.05	100.06	99.48	100.27	99.94	99.29	100.61	100.15	99.19	99.41
L.O.I.	0.64	2.03	0.20	1.22	0.73	2.93	3.31	0.38	3.45	0.54	3.12	0.31	1.90	0.26	2.03	0.40	1.40	1.39	2.38
FeO ^{total}	6.66	3.57	7.59	4.38	6.78	4.78	4.78	6.54	6.12	5.83	5.21	5.21	5.99	6.49	5.43	6.79	4.65	6.18	6.17
Mg#	75.01	74.18	75.22	76.96	73.15	73.58	76.36	76.97	76.15	77.58	76.52	78.92	77.82	77.44	74.00	80.95	77.76	78.91	78.81
Fe ³⁺ /Fe ^{total}	n.d.	0.406	0.139	0.296	0.232	n.d.	0.375	0.137	0.381	0.178	0.384	0.171	0.369	0.196	0.338	0.177	0.304	0.199	0.159
Trace element concentration (ppm)																			
Li	3.45	5.18	3.76	4.53	6.26	6.62	8.15	3.88	28.64	5.15	38.00	3.95	6.34	3.18	3.77	3.75	9.78	1.18	1.62
Be	0.11	0.17	0.12	0.13	0.23	0.24	0.22	0.12	0.11	0.15	0.14	0.08	0.06	0.13	0.23	0.08	0.12	0.08	0.17
Sc	44.7	19.9	43.2	41.8	39.2	39.8	40.7	26.9	38.6	37.4	26.8	35.4	40.1	45.0	36.6	51.2	33.9	30.4	34.4
V	164	71	166	161	159	138	152	106	133	140	102	123	137	173	131	192	126	104	119
Cr	82	33	66	64	154	131	143	170	205	135	92	157	193	104	79	325	209	185	233
Co	41.7	26.2	51.6	28.2	40.0	29.4	27.3	50.4	43.3	42.2	40.1	39.4	47.3	44.9	35.6	53.1	35.1	49.4	46.1
Ni	79.2	47.5	90.2	49.4	95.7	73.9	66.3	117.9	106.7	116.2	107.4	95.5	120.3	95.2	77.9	130.4	99.1	136.1	133.1
Cu	80.4	36.1	67.2	63.5	67.0	46.5	41.6	41.2	60.4	115.2	86.3	68.4	96.7	67.3	47.1	43.9	78.6	90.9	31.5

(Continued)

Table 3. (Continued)

Sample Depth	F10	A10	F11	A11	F12	A12-1	A12-2	F13	A13	F14	A14	F15	A15	F16	A16	F17	A17	F18	A18
	1133.02	1133.63	1139.05	1138.75	1183.61	1183.73	1183.81	1207.41	1207.57	1235.75	1235.92	1316.00	1316.39	1327.95	1328.23	1476.27	1475.96	1493.27	1493.67
Zn	33.3	21.4	38.6	24.4	43.2	30.3	27.5	36.3	31.5	31.5	30.0	30.0	29.2	35.9	33.4	37.5	25.3	31.5	25.7
Ga	11.9	15.0	11.8	14.2	13.4	12.7	12.6	11.7	11.6	12.1	12.1	11.8	11.4	11.9	13.9	8.8	12.0	11.2	10.8
Rb	0.13	0.82	0.10	0.12	0.14	0.93	0.79	0.08	0.41	0.23	0.75	0.08	0.22	0.15	0.20	0.06	0.31	0.15	0.24
Sr	146.3	212.9	142.0	177.6	164.3	169.8	175.4	167.4	139.5	158.2	167.9	167.1	143.6	148.8	171.6	107.4	176.7	151.0	142.3
Sr	142.8	209.9	139.3	174.5	158	166.8	172.3	160.5	134.6	150.9	161.4	155.5	135.1	148.9	160	105.8	175.3	148.6	141.6
Y	9.7	4.9	11.2	10.4	13.1	11.9	13.3	6.6	8.7	10.7	7.6	6.7	7.1	11.8	12.2	10.9	8.6	6.0	7.0
Zr	13.2	7.5	16.9	12.6	26.4	25.0	25.2	11.1	17.8	34.5	33.3	6.8	5.6	27.6	24.1	16.0	15.0	7.6	6.5
Nb	0.125	0.116	0.127	0.109	0.443	0.333	0.198	0.105	0.207	0.522	0.609	0.046	0.034	0.169	0.154	0.135	0.136	0.078	0.134
Cs	0.001	0.001	0.001	0.002	0.001	0.008	0.001	0.002	0.056	0.003	0.042	0.001	0.003	0.003	0.013	-0.001	0.000	0.001	0.001
Ba	2.68	8.67	2.20	2.96	3.13	4.62	5.45	2.02	1.63	3.80	11.57	1.84	1.77	2.20	3.28	1.16	4.28	1.68	2.50
Ba	2.80	9.23	13.68	3.02	3.28	4.59	5.31	1.90	1.36	4.09	12.57	1.44	1.66	3.06	3.00	1.24	4.24	1.65	2.13
La	0.49	0.58	0.58	0.54	0.87	1.01	1.00	0.52	0.98	1.13	1.02	0.35	0.26	0.90	1.09	0.45	0.61	0.37	1.02
Ce	1.85	1.66	2.19	1.90	3.10	3.35	3.37	1.74	2.23	3.69	3.09	1.16	1.00	3.24	3.62	1.82	2.07	1.26	2.45
Pr	0.38	0.28	0.45	0.39	0.61	0.62	0.64	0.32	0.42	0.65	0.51	0.24	0.22	0.61	0.67	0.39	0.39	0.25	0.47
Nd	2.27	1.49	2.69	2.32	3.43	3.39	3.58	1.83	2.29	3.37	2.54	1.46	1.42	3.40	3.63	2.39	2.22	1.46	2.41
Sm	0.99	0.52	1.13	1.01	1.40	1.29	1.38	0.70	0.90	1.18	0.83	0.64	0.66	1.31	1.35	1.06	0.88	0.59	0.82
Eu	0.58	0.55	0.59	0.63	0.77	0.72	0.75	0.50	0.54	0.59	0.59	0.47	0.45	0.61	0.72	0.50	0.53	0.43	0.44
Tb	0.27	0.13	0.31	0.28	0.37	0.33	0.37	0.18	0.24	0.30	0.21	0.19	0.20	0.33	0.34	0.31	0.24	0.16	0.20
Gd	1.48	0.73	1.68	1.54	1.99	1.83	1.99	1.01	1.32	1.64	1.18	1.00	1.03	1.85	1.90	1.64	1.29	0.91	1.12
Dy	1.83	0.89	2.09	1.91	2.50	2.23	2.45	1.22	1.63	2.02	1.41	1.27	1.34	2.24	2.26	2.05	1.62	1.13	1.35
Ho	0.39	0.19	0.45	0.41	0.53	0.48	0.52	0.27	0.35	0.43	0.30	0.27	0.29	0.48	0.49	0.44	0.35	0.24	0.29
Er	1.10	0.53	1.26	1.15	1.49	1.34	1.47	0.75	0.97	1.21	0.84	0.74	0.78	1.33	1.38	1.24	0.96	0.67	0.81
Tm	0.16	0.08	0.19	0.17	0.22	0.20	0.22	0.11	0.15	0.18	0.12	0.11	0.12	0.19	0.20	0.18	0.14	0.10	0.12
Yb	1.01	0.49	1.16	1.04	1.38	1.26	1.36	0.67	0.91	1.13	0.80	0.69	0.73	1.22	1.27	1.11	0.87	0.61	0.77
Lu	0.15	0.07	0.17	0.15	0.21	0.19	0.20	0.10	0.14	0.17	0.12	0.10	0.11	0.18	0.19	0.17	0.13	0.09	0.11
Hf	0.469	0.245	0.567	0.467	0.820	0.781	0.818	0.337	0.538	0.921	0.729	0.275	0.256	0.815	0.774	0.556	0.468	0.278	0.249
Ta	0.010	0.010	0.011	0.013	0.036	0.028	0.024	0.014	0.015	0.073	0.067	0.004	0.003	0.023	0.013	0.013	0.012	0.005	0.013
Pb	0.313	0.258	0.184	0.179	0.277	0.363	0.317	0.498	0.175	0.306	0.303	0.198	0.201	0.189	0.338	0.111	0.295	0.159	0.277
Th	0.010	0.010	0.012	0.011	0.013	0.019	0.026	0.011	0.017	0.040	0.041	0.005	0.004	0.016	0.009	0.010	0.012	0.006	0.012
U	0.004	0.007	0.005	0.005	0.005	0.007	0.011	0.004	0.006	0.018	0.018	0.001	0.001	0.006	0.003	0.004	0.004	0.002	0.006
$\delta^{18}\text{O}$					5.96	8.71	8.55	6.41	8.14									4.42	4.73
87Sr/86Sr	0.702818	0.702902	0.702887	0.702902	0.702841	0.702942	0.702922	0.702815	0.702874	0.702811	0.702935	0.702821	0.702809	0.702790	0.702843	0.702829	0.702816	0.702786	0.702

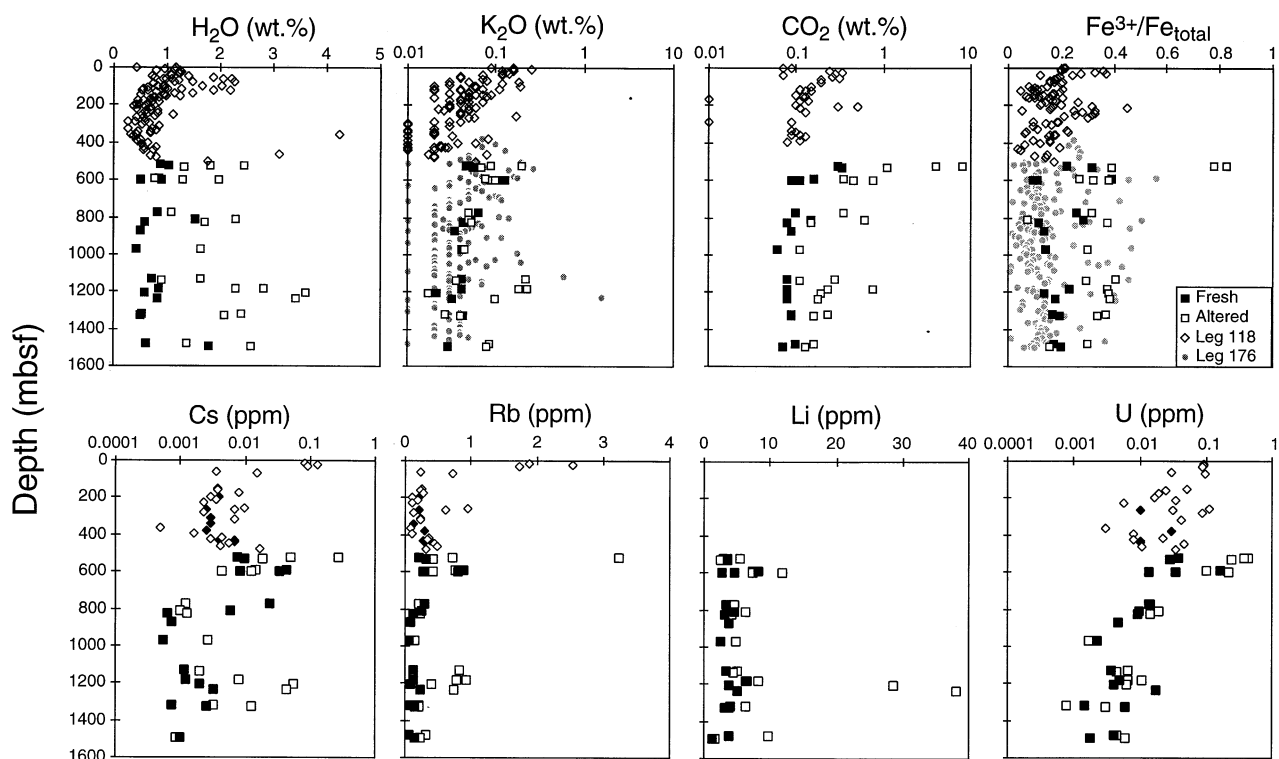


Fig. 5. Downhole variation of alteration-sensitive major and trace components and the degree of oxidation. Leg 118 and Leg 176 shipboard data (Von Herzen et al., 1989; Shipboard Scientific Party, 1999) and trace element data from Hart et al. (1999) are plotted in addition to data from this study. Altered samples generally exhibit higher concentrations of H_2O , K_2O , and CO_2 , and reveal larger extents of oxidation than their fresh counterparts. The Leg 118 data seem to suggest decreasing H_2O and K_2O contents from 0 to 500 mbsf. This would be expected if low-T alteration (seafloor weathering) was restricted to shallowest part of the basement. The combined data sets, however, suggest there is no systematic trend of decreasing alteration down the hole. Highs in alkali, U, H_2O , and CO_2 concentrations and in the degree of oxidation occur at certain depth levels where alteration is locally enhanced along low-grade metamorphic veins. Li is most strongly enriched in two nonoxidatively altered samples from between 1200 and 1250 mbsf.

uppermost 500 mbsf into two low-temperature alteration zones (Table 2). Zone 1' is characterized by oxidative alteration, whereas zone 2' exhibits only weak, nonoxidative low-grade alteration. The overall extent of low-grade alteration is small, with only around 2% of the igneous core material transformed into low-grade secondary minerals.

3.2. Chemical and Isotopic Compositions

3.2.1. Downhole Trends

Downhole variations in the chemistry of fresh/alter sample pairs are presented in Table 3, and displayed in Figure 5 in comparison with bulk rock samples from the uppermost 500 m. A comparison with the abundance of low-grade metamorphic veins (Fig. 2C) shows that increases in water content are highest in highly veined areas. Large increases in K_2O concentrations are confined to the oxidatively altered zone 1 (500–600 mbsf) and zone 4 (1050–1300 mbsf). CO_2 contents throughout the hole are above those typically found in oceanic gabbros (0.02 wt.%; Alt and Teagle, 1999). CO_2 enrichment in the altered rocks is highest in the oxidatively altered zone 1. One source of CO_2 is calcite veins, which are clearly visible in zone 1. However, even below the depth of macroscopic calcite veins

(around 700 mbsf), CO_2 is enriched in the altered rocks relative to the fresh precursors. Thin-section observations (Table 1) confirm the presence of calcite in microscopic veinlets.

The fractions of ferric iron are generally higher than those typical of fresh mid-ocean ridge basalt (MORB) glasses (0.07 ± 0.03 ; Christie et al., 1986). With the exception of the most S-rich sample (132R1, 70–78 cm; 1.18 wt.% S) and the greenschist-facies altered rock from near the bottom of the hole, all altered rocks have higher oxidation states than the “fresh” precursors. This includes samples with abundant secondary pyrite, suggesting the pyrite was formed under fairly oxidizing conditions, possibly involving sulfate-reducing bacteria (Alt and Shanks, 1998). Both Rb and Cs show significant enrichments in zones 1 and 4, similar to K. In contrast, large Li enrichments appear to be confined to zone 4. U concentrations seem to decrease downhole, consistent with the overall trend of decreasing incompatible element content with increasing depth (Dick et al., 2000). Strong U enrichments are confined to the oxidatively altered rocks in zone 1.

Figure 6 depicts the downhole variations in O and Sr isotopic composition. In the upper 200 mbsf, $\delta^{18}\text{O}$ values systematically lower than magmatic values (shaded area in Fig. 6) can be accounted for by more or less pervasive amphibolite facies

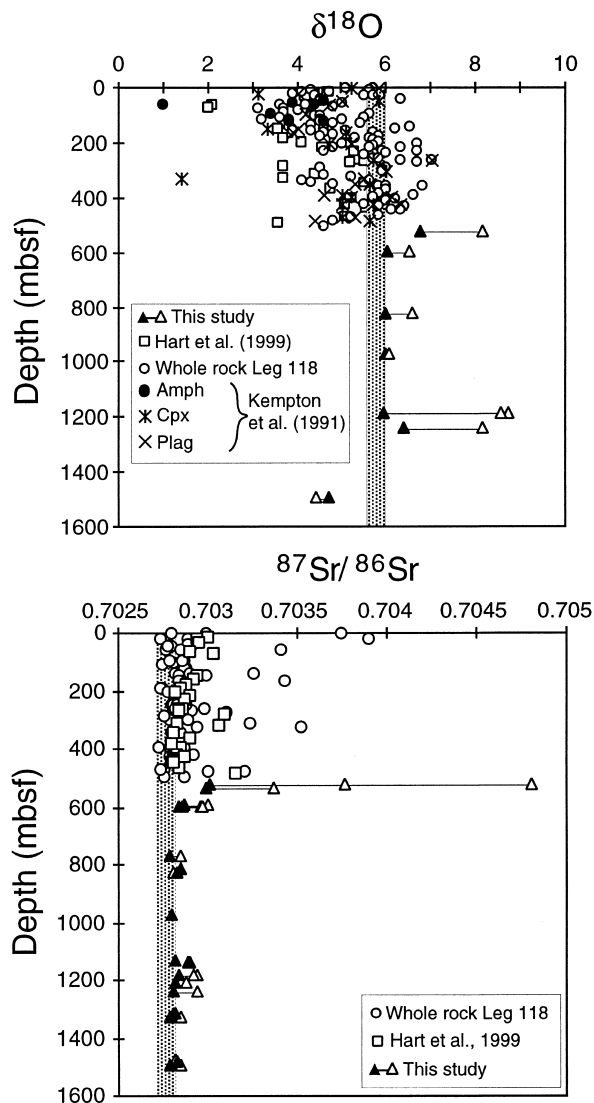


Fig. 6. Downhole variation of O and Sr isotope compositions of rocks and minerals in Hole 735B. Open circles represent whole rock data for the Leg 118 section from Stakes et al. (1991) and Kempton et al. (1991); open squares mark strip samples from Hart et al. (1999). Note that $\delta^{18}\text{O}$ is generally lower than magmatic values ($5.7 \pm 0.2\text{‰}$ —shaded area) shallow in the hole, owing to the high intensity of amphibolite-facies alteration. In contrast, low-grade altered samples from deeper in the hole have increased $\delta^{18}\text{O}$ values compared to their fresh counterparts. The sample pair from near the bottom of the hole represents greenschist-facies alteration with temperatures of water/rock interaction being high enough to result in ^{18}O depletion of the rock. Sr isotope ratios of fresh and altered pairs are fairly uniform deep in the hole, with only subtle enrichments in $^{87}\text{Sr}/^{86}\text{Sr}$ in the most intensively altered rocks from around 1200 mbsf (zone 4). In contrast, the oxidatively altered rocks from zone 1 (500–600 mbsf) exhibit some of the highest $^{87}\text{Sr}/^{86}\text{Sr}$ ratios reported for Hole 735B. Variability in $^{87}\text{Sr}/^{86}\text{Sr}$ in the uppermost 500 mbsf has been explained by varying degrees of greenschist and amphibolite-facies alteration developed in zones of increased ductile and brittle deformation.

alteration. Except for low $\delta^{18}\text{O}$ ratios around 300 mbsf and near 500 mbsf, most of the whole rock $\delta^{18}\text{O}$ values are similar to fresh MORB glasses ($5.7 \pm 0.2\text{‰}$; Ito et al., 1987). The $\delta^{18}\text{O}$ minimum at 300 mbsf is due to increased greenschist facies

alteration in the vicinity of hydrothermal breccias; the low $\delta^{18}\text{O}$ ratios near 500 mbsf correspond to an increase in the abundance of amphibole (cf. Fig. 2B). Due to the low abundance of high-temperature alteration deep in the hole, low $\delta^{18}\text{O}$ values are rare at depth and are restricted to the greenschist facies altered rocks from below 1475 mbsf. This suggests that high-temperature fluid ingress was very limited below ~ 600 mbsf, consistent with the near absence of amphibole as a secondary phase below this depth. Locally abundant low-grade alteration, however, resulted in ^{18}O enrichment in parts of deep basement at Site 735. Hence, the O isotopic profile for the plutonic section of Hole 735B is the reverse of that typically seen for “normal” oceanic crust, where permeability and integrated water-to-rock ratios decrease and peak alteration temperatures increase downward, leading to ^{18}O enrichments in the shallow crust and ^{18}O depletions in the high-temperature altered deeper crust (Muehlenbachs and Clayton, 1972a, 1972b; Alt et al., 1996; Elthon et al., 1984; Gregory and Taylor, 1981).

Elevated $^{87}\text{Sr}/^{86}\text{Sr}$ ratios in the uppermost 500 m of the hole have been explained by extensive high-temperature alteration (Kempton et al., 1991). Because the effect of low-grade alteration on Sr isotope composition is generally minor (Fig. 6), the Sr isotope profile is not as variable as the O isotope profile, with the exception of high $^{87}\text{Sr}/^{86}\text{Sr}$ ratios in the carbonate-rich oxidatively altered zone 1.

3.2.2. Effect of Alteration

A summary of the principal mineralogical and compositional changes associated with low-grade alteration in Hole 735B is given in Table 2. Element concentrations, fractions of ferric iron (a proxy for the degree of oxidation), and Sr and O isotopic compositions of fresh and altered samples have been plotted against the estimated degree of alteration (expressed as percent secondary phases) in Figures 7 and 8.

Consistent with the replacement of primary minerals by smectites or chlorite/smectite mixed-layer phases and carbonate, the trends displayed in Figure 7 suggest a general decrease in SiO_2 content with increasing alteration, and variable increases and decreases in MgO and CaO contents. As a result of alteration and formation of phyllosilicates, all altered samples gained considerable amounts of H_2O (up to 3.5 wt.%). K_2O , CO_2 , and S contents, and the fraction of ferric iron generally increased with increasing alteration. Sulfur exhibits lower concentrations in some of the most oxidized rocks, and K_2O enrichment is variable. Changes in Li contents during alteration range from very subtle increases to strong enrichments (Fig. 8). Similar behavior is observed for Rb, Cs, and U, although variations in these elements do not correlate well with changes in Li contents.

Elemental changes are most pronounced in zones 1 and 4 where alteration is most intense. An overview of the changes in trace element composition for representative fresh/alterated sample pairs from the most intensely altered zones 1 and 4 is presented in the form of “spidergrams” in Figure 9. Rocks from zone 1 are strongly enriched in Rb, Cs, K, U, and P. In contrast, enrichment in these elements is much more subtle in rocks from zone 4 that show pronounced Li enrichment. Enrichments in K, Rb, Cs, U, and P have also been reported for gabbros from the uppermost 40 mbsf drilled during Leg 118 (Hart et al., 1999).

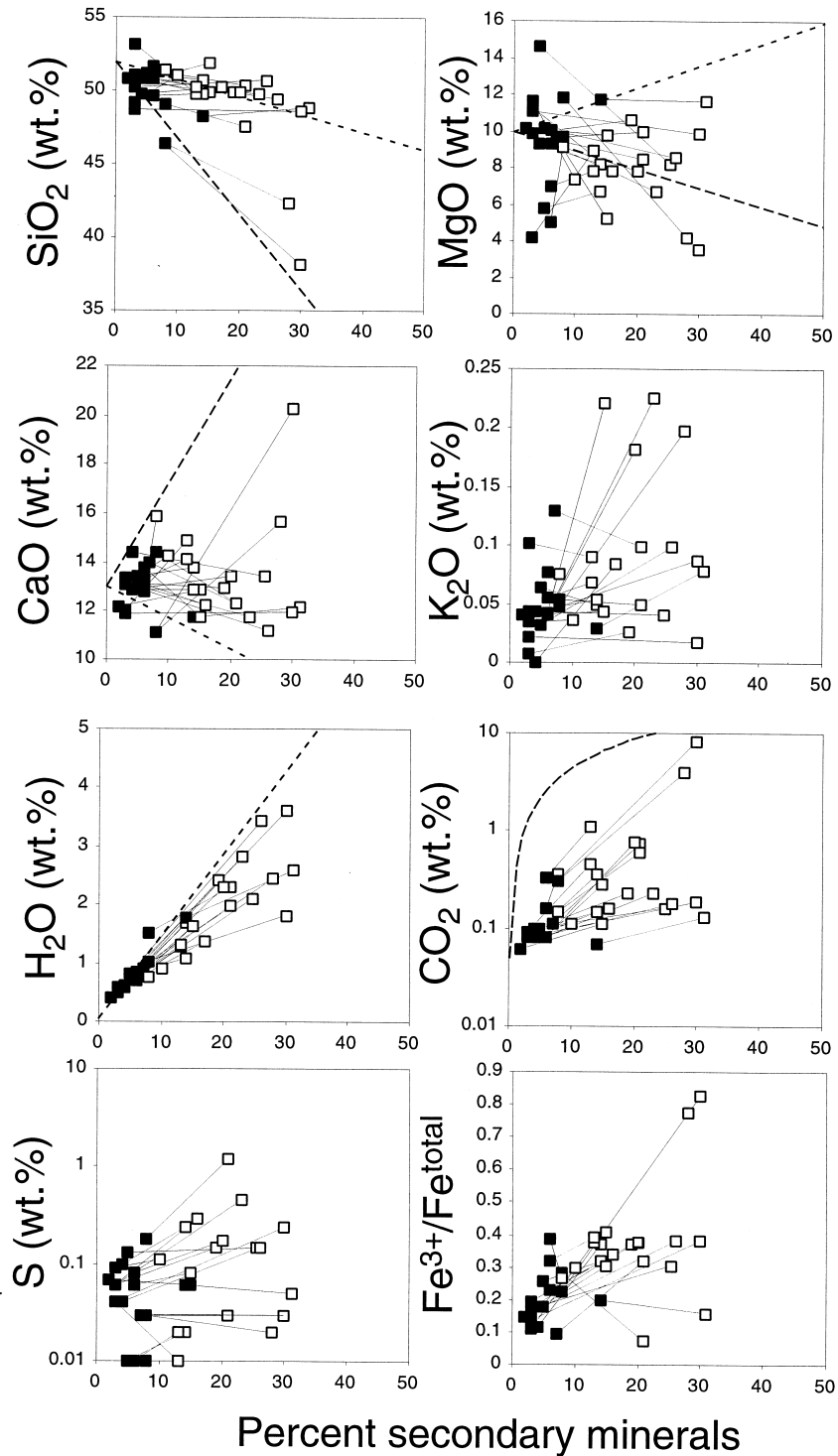


Fig. 7. Plots of major element concentrations versus the estimated degree of alteration (% secondary phases). Symbols as in Figure 3. Dashed lines are trends resulting from replacing the rock by saponite (short dashes) and calcite (long dashes). Note that the most common replacement of igneous phases by clays, chlorite, and subordinate calcite results in decreases in the concentrations of Si, Mg, and Ca, whereas K, H₂O, and CO₂ contents generally increase. In many examples, sulfur concentrations appear to increase as a result of alteration and partial replacement of olivine by secondary sulfides, although decreasing S contents are also observed, particularly in the most oxidized rock. Alteration results generally in an uptake of oxygen, as expressed by increasing Fe³⁺/ΣFe.

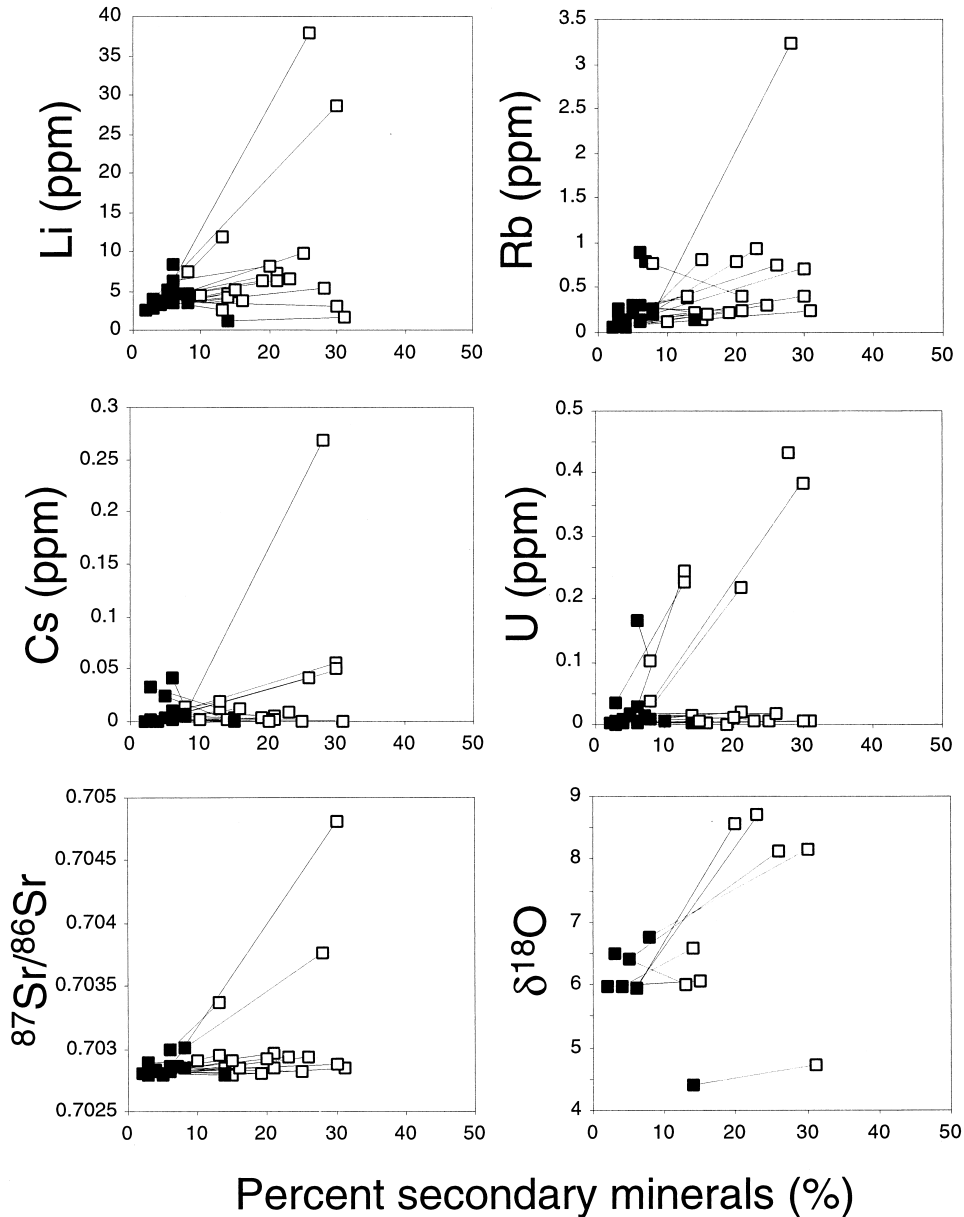


Fig. 8. Plots of trace element concentrations and Sr and O isotope compositions versus degree of alteration. Altered rocks show increases in Li, Rb, Cs, U, ^{87}Sr , and ^{18}O concentrations relative to their fresh counterparts. The extents of enrichment for Rb, Cs, U, and ^{87}Sr range from subtle in the nonoxidatively altered rocks to strong in the oxidatively altered rocks.

Enrichments in alkalis and U are among the most distinct characteristics of oceanic basaltic rocks altered at low temperature under oxidizing conditions (Thompson, 1983; Hart and Staudigel, 1982; Teagle et al., 1996). Previous work has shown that smectite (mainly saponite) is often enriched in Li, probably due to replacement of Mg by Li in the octahedral sites of smectite (Berndt and Seyfried, 1986). Smectites are also often enriched in K, Rb, and Cs owing to their great ion exchange capacity. Typically, the enrichments factor increases in the order of $\text{K} < \text{Rb} < \text{Cs}$ (Hart and Staudigel, 1982), which reflects a decrease in free energies of hydration of alkalis in the same order (Berger et al., 1988). Micas, such as celadonite, have a much smaller ion exchange capacity than smectites, but

have alkalis stoichiometrically incorporated in their interlayer sites. In the gabbroic section from Hole 735B, enrichment of K, Rb, and Cs in zone 1 is most likely related to celadonite layers in smectite and to nontronite, for which electron microprobe analyses have revealed high K concentrations (Alt and Bach, 2001). Li is not enriched in zone 1, suggesting that ferric clays and micas did not take up significant amounts of Li along with the larger alkali ions. Li enrichment in zone 4 is probably related to the substitution of Li for Mg in the octahedral sites of Mg-rich saponite. Mild to moderate enrichment of K, Rb, and Cs below 600 mbsf can be explained by limited uptake of these elements by smectite.

The 10-fold enrichment of U in zone 1 is remarkable. U

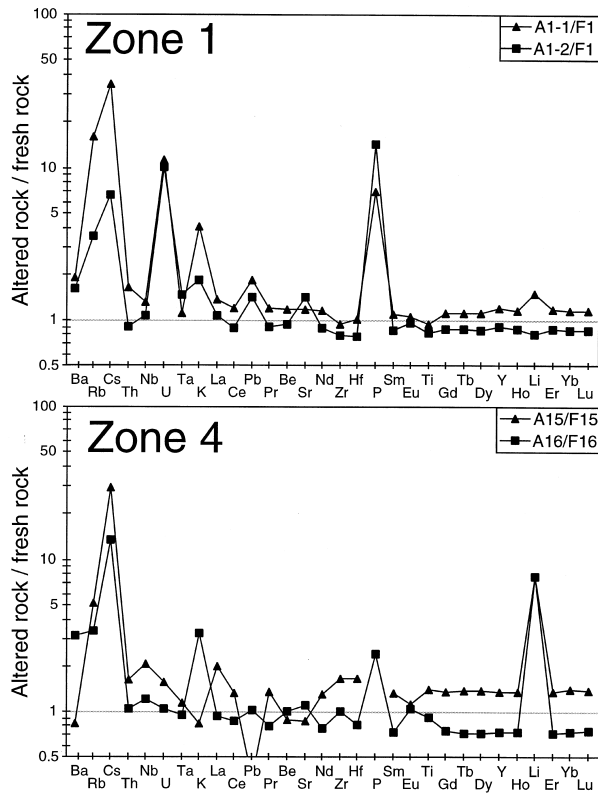


Fig. 9. Trace element distribution diagrams (spidergrams) for representative fresh/altered sample pairs from zone 1 and zone 4. Plotted are element concentrations of the altered rock divided by that of the fresh precursor. Elements are plotted from right to left in the order of increasing incompatibility during mantle melting (Niu and Batiza, 1997).

concentrations in 735B gabbros are compared to basalts from various locations in Figure 10. U concentrations in oxidatively altered gabbros from zone 1 in Hole 735B are higher than in rocks from drill holes (504B, 896A) in a 6-Ma volcanic ridge flank in the eastern equatorial Pacific and similar to, or slightly lower than, in basalts formed at the Mid-Atlantic Ridge. Different hosts for U in low-temperature altered rocks have been proposed. Aumento (1971) observed a positive correlation between U and the degree of oxidation (Fig. 10A), and proposed Fe oxyhydroxides or clays as the primary U hosts in oxidatively altered basalts. Hart and Staudigel (1986) found very low U concentrations in celadonite and celadonite/smectite phases, and Porter et al. (2000) reported similarly low U concentrations for saponites from Juan de Fuca Ridge flank basalts. These data hence suggest that Fe oxyhydroxides may be the most likely U site. Fe oxyhydroxides can also explain the enrichment of P in rocks from zone 1, as P is effectively adsorbed on Fe oxyhydroxides (Berner, 1973).

Based on a loose correlation between U and CO_2 at Sites 417 and 418 (Fig. 10C), Staudigel et al. (1996) argued that U may be hosted by calcite. U concentrations in four calcite separates from veins in Hole 735B between 500 and 600 mbsf range from 0.14 to 0.19 ppm (Alt and Bach, 2001). These results suggest that carbonates, although enriched in U relative to the fresh rock, cannot explain the observed U enrichment in the altered rocks in Hole 735B (Fig. 10D). Carbonates would have to

contain ~ 10 times more U to account for the U excess in the rocks. Using an average $D^{\text{Ca-U}}$ of 0.3 (Rihs et al., 2000), U in calcite would be predicted to be around 1 ppm, if the Ca/U ratio of seawater is assumed. Because any fluid/rock reaction would increase Ca and decrease U, the observed low U concentrations in the calcites suggest that the fluids from which the carbonate precipitated had reacted with the basement to some extent.

O isotope data suggest gains in ^{18}O in most of the altered rocks (Fig. 8). The one exception is a sample pair from near the bottom of the hole for which low $\delta^{18}\text{O}$ values suggest high alteration temperatures ($>250^\circ\text{C}$). This is consistent with the greenschist-facies alteration assemblage observed in rocks from >1475 mbsf.

$^{87}\text{Sr}/^{86}\text{Sr}$ ratios in most of the altered rocks are only marginally elevated compared to the fresh precursor (Fig. 8). Only carbonate-bearing rocks from zone 1 show distinct ^{87}Sr enrichments. Figure 11 depicts $^{87}\text{Sr}/^{86}\text{Sr}\text{-H}_2\text{O}$ and $^{87}\text{Sr}/^{86}\text{Sr}\text{-CO}_2$ relationships of 735B gabbros in comparison with those of altered basaltic rocks from volcanic ridge flanks. A simple mixing model can account for the elevated $^{87}\text{Sr}/^{86}\text{Sr}$ in the carbonate-bearing rocks from zone 1, if it is assumed that the calcites have 400 ppm Sr with $^{87}\text{Sr}/^{86}\text{Sr} = 0.709$ (Fig. 11A). This Sr concentration and isotopic composition assumed for the calcite are similar to those obtained for vein calcites from zone 1 (Alt and Bach, 2001). Sr isotope ratios for chlorite/smectites mixed-layer phases and smectites range from 0.70312 to 0.70543, and $^{87}\text{Sr}/^{86}\text{Sr}$ for phyllosilicates from below 1200 mbsf are <0.7035 (Alt and Bach, 2001). The range in $^{87}\text{Sr}/^{86}\text{Sr}$ ratios measured for vein smectite is low compared to the values reported for saponites from ODP Holes 896A and 504B in which $^{87}\text{Sr}/^{86}\text{Sr}$ range from 0.7032 to 0.7090 (Teagle et al., 1998). Sr concentrations in the clays from Hole 735B are low, typically around 40 ppm (Alt and Bach, 2001). Figure 11B shows that the “carbonate-free” bulk rock samples from Hole 735B plot along a mixing line between fresh gabbro and smectite characterized by similarly low Sr concentrations and $^{87}\text{Sr}/^{86}\text{Sr}$.

Although these simple mixing models provide a first-order explanation for the Hole 735B Sr isotope data, interpretation of the Sr data for basaltic sections from volcanic ridge flanks is more ambiguous. Formation of both carbonate and clay must be important in setting the $^{87}\text{Sr}/^{86}\text{Sr}$ of the altered basaltic rocks on ridge flanks. At a given CO_2 or H_2O concentration, basalts from deep drill holes have higher $^{87}\text{Sr}/^{86}\text{Sr}$ than gabbros from 735B. This may indicate a greater component of seawater-derived Sr in altered rocks from volcanic ridge flanks. Low Sr isotope ratios for the majority of the Hole 735B samples suggest that fluid circulation was fairly restricted and overall water-to-rock ratios were small. Alternatively, the fluids in Hole 735B could have lost a large fraction of seawater Sr due to precipitation of aragonite or anhydrite.

3.3. Magnitude and Direction of Chemical Change

We have used the differences between the concentrations of elements in altered rocks (C_A) and those in corresponding fresh rocks (C_F) to derive alteration-related mass changes for various elements. These calculations were done in a series of steps. First, we assumed that TiO_2 was immobile during alteration and normalized the element concentrations in the altered rocks

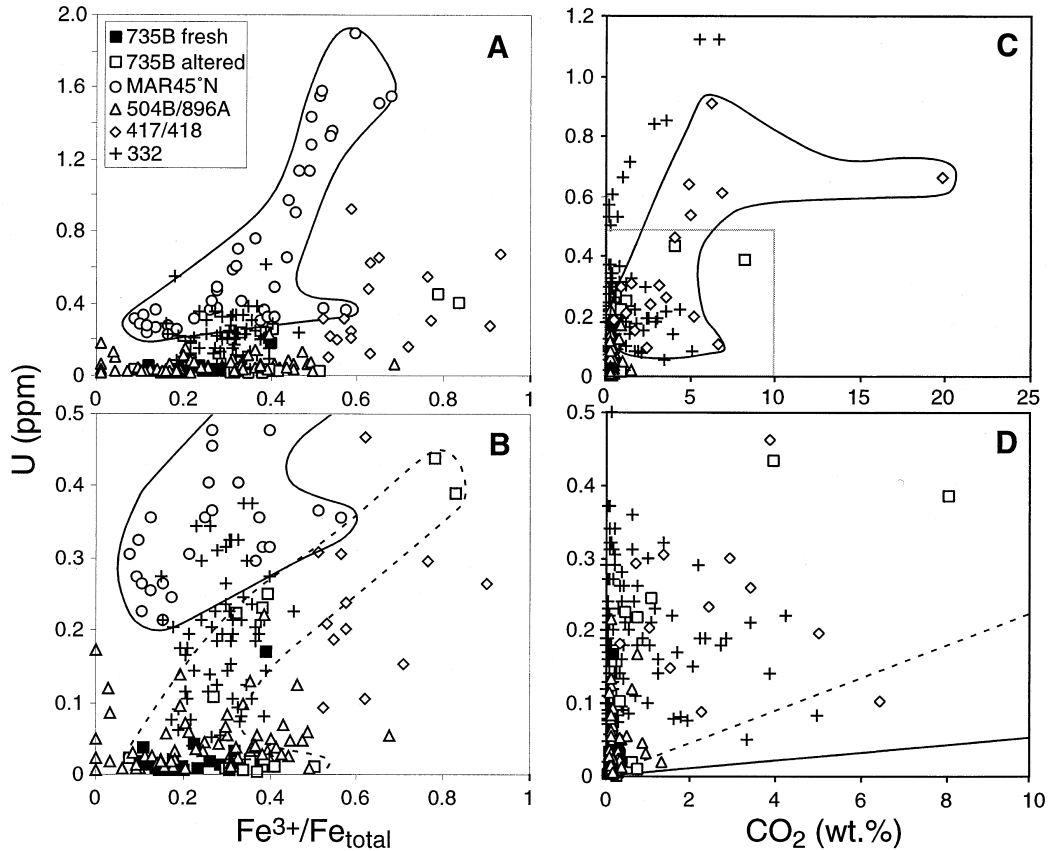


Fig. 10. Concentration of U versus the degree of oxidation and CO₂. Note that panels B and D are blow-ups of the diagrams shown in A and C, respectively. Envelopes with solid lines encompass data from the Mid-Atlantic Ridge at 45°N in A and B, and data from DSDP Sites 417 and 418 in C. The envelope with the dotted line in B encompasses data from this study. Lines in Figure 10D are mixing lines of fresh rock with Hole 735B calcite (0.15 ppm U; solid line) and hypothetical calcite precipitated from seawater (1 ppm; dashed line). Data sources are: Aumento (1971), Teagle et al. (1996), Staudigel et al. (1996), Mitchell and Aumento (1977), and Bach (unpublished).

(Table 3) to the same TiO₂ content of its fresh rock precursor. The relation between the concentration change between fresh and alteration rock ($\Delta C = C_A - C_F$) and the degree of alteration was then used to derive ΔC per percent alteration for the different alteration zones (Table 4). To include the uppermost 500 m of the drillhole, it was assumed that the relationships between chemical changes and degree of alteration were similar to comparable zones from deeper levels (Table 4), and then the visually estimated degree of low-grade background alteration (Fig. 4) was used to derive ΔC per percent alteration for the different alteration zones. Finally, ΔC was integrated over the entire depth interval to calculate mass changes for individual elements for the entire drilled section (Table 5).

It is instructive to compare potential chemical changes for the lower crust (as represented by the gabbroic section at Hole 735B) with those calculated for drilled basaltic sections recovered from Deep Sea Drilling Project (DSDP) Sites 417/418 in 110-Ma crust in the North Atlantic (Staudigel et al., 1996), and from DSDP/ODP Hole 504B in a 6-Ma ridge flank located 200 km south of the Costa Rica Rift Zone in the equatorial East Pacific (Alt et al., 1996), even though there are large uncertainties associated with such calculations for rocks recovered from holes drilled in ridge flanks [see discussions in Alt et al.

(1996) and Alt and Teagle (1999)] (Table 5). Such a comparison shows that the direction of chemical change is similar, with both kinds of crust acting as sink for the alkalis, H₂O, C, P, and U. In general, chemical changes derived for Hole 735B-like crust are an order of magnitude or more lower than changes inferred for basaltic crust. This difference likely reflects the overall lower degree (by about an order of magnitude) of low-grade alteration in Hole 735B (ca. 2%) compared with that found in volcanic rocks from normal ridge flanks (Alt et al., 1996). The magnitude of changes estimated for MgO, Na₂O, P₂O₅, and CO₂ is similar, or only slightly lower, than estimates for volcanic ridge flanks. However, our data suggest that uplifted lower ocean crust provides a sink for sulfur, in contrast to volcanic ridge flanks, where the upper volcanics appear to have lost a significant fraction of S due to oxidation of magmatic sulfides (Alt, 1995).

A particularly interesting result is that low-T alteration of uplifted lower crust appears to act as a source of Mg to the oceans. It has been previously shown that breakdown of olivine during seafloor weathering leads to Mg loss from basalts (Thompson, 1973; Alt and Honnorez, 1984). Results from ODP Holes 504B and 896A reveal that despite a Mg loss from the altered basalt, more Mg is gained during the formation of

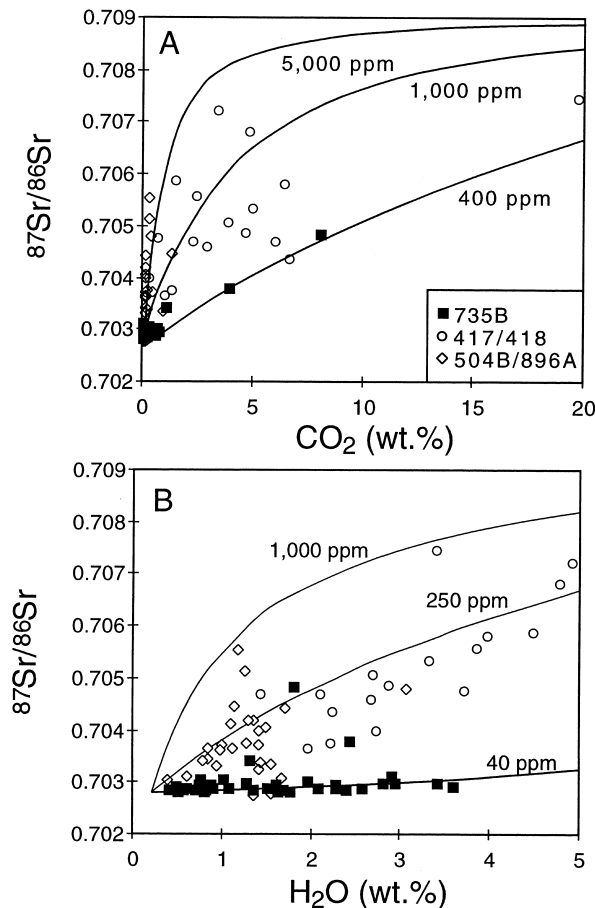


Fig. 11. Plots of $^{87}\text{Sr}/^{86}\text{Sr}$ ratios versus CO_2 (A) and H_2O (B) concentrations. Lines represent mixing lines calculated for mixtures between fresh rock and calcite (A) and smectite (B). Different lines are plotted for different Sr concentrations of calcite and smectite, respectively. Assumptions of the mixing models are: $^{87}\text{Sr}/^{86}\text{Sr}$ in fresh rocks = 0.7028, $^{87}\text{Sr}/^{86}\text{Sr}$ in Hole 735B smectite = 0.7035, $^{87}\text{Sr}/^{86}\text{Sr}$ in smectite replacing basalt = 0.7086, $^{87}\text{Sr}/^{86}\text{Sr}$ in carbonate = 0.709, [Sr] in Hole 735B gabbros = 160 ppm, [Sr] in basalts = 80 ppm. Basalt data sources are: Teagle et al. (1996), Staudigel et al. (1996), Barrett (1983), and Kawahata et al. (1987).

clay-rich veins and breccia cement; consequently, the crust is a net sink for Mg (Alt et al., 1996). Hence, the role of smectite veins in the Mg budget calculated for Site 735 needs to be evaluated. In the lower 1 km of Hole 735B, smectite veins comprise 0.08% of the core volume (Shipboard Scientific Party, 1999), which is only 5 to 10% of that observed in Holes 504B and 896A. Using an average MgO concentration of smectite of 21 wt.% (Alt and Bach, 2001), the Mg uptake related to the formation of smectite veins for the entire drilled section is 0.017 g MgO/100g of rock. This is only $\sim 10\%$ of the estimated Mg loss from the rock, suggesting that the formation of smectite veins had insignificant consequences for the Mg budget for Hole 735B. Hence, it appears that low-T alteration of mafic plutonic rocks might provide a small source of Mg to the oceans.

Similar to the effect of smectite veins on the Mg budget, the proportion of macroscopic calcite veins (0.04% of the core volume) is too small to significantly impact the mass changes

calculated for CO_2 . Accounting for the presence of calcite veins increases the calculated CO_2 mass change by 30%. Overall, the concentrations of CO_2 in Hole 735B are high compared to the very low abundance (≤ 0.02 wt.%) reported for gabbros from the MARK area (Mid-Atlantic Ridge near the Kane Fracture Zone at 23°N) and from Hess Deep (Shipboard Scientific Party, 1993, 1995). Because CO_2 is elevated in portions of the drill core that are apparently devoid of carbonates, it is possible that the elevated background concentration of CO_2 in Hole 735B is in part related to other sources of carbon, such as methane-rich fluid inclusions or graphite (Kelley, 1996; Kelley and Früh-Green, 1999; Vanko and Stakes, 1991). The difference in CO_2 contents between “fresh” and “altered” sample pairs, however, is most likely the result of a greater abundance of microscopic carbonate veins in the altered rocks.

It is interesting to note that the crust at Site 735 is older (11.9 Ma; John et al., 2001) than the crustal sections drilled in the MARK and Hess Deep areas (< 1 Ma). This may indicate that uptake of C by exposed plutonic crust is a continuous process. Similarly, Alt and Teagle (1999) have speculated that C uptake by the crust may generally be continuous. Fluxes of C calculated for Holes 504B/896A (Alt et al., 1996) and the Juan de Fuca Ridge flank (Sansone et al., 1998; Wheat and Mottl, 2000) are about an order of magnitude lower than those calculated based on carbonate abundance at DSDP Sites 417/418 (Staudigel et al., 1989), as well as at Sites 801 (800 km E of the Mariana Trench) and 843 (225 km SW of the island of Oahu) (Alt and Teagle, 1999). Whereas the Juan de Fuca Ridge flank and Holes 504B/896A represent young ridge flanks where rapid sedimentation rates result in conductive reheating of the shallow basement (i.e., they are “warm” flanks), the sites for which larger C fluxes have been inferred are situated in old crust (110–165 Ma). Hence, the differences in mass changes in C can be accounted for if C uptake is not restricted to crust less than 10 to 15 Ma, as suggested by Staudigel et al. (1981) and Richardson et al. (1980), but continues in crust of much older age (Alt and Teagle, 1999). Alternatively, the difference in C uptake could be related to differences in sedimentation rates and thermal evolution of “warm” and “cold” ridge flanks. The distinctly greater C uptake calculated for the gabbros at Site 735 compared to gabbros from drill holes in younger crust strongly suggests that C uptake continued after the lower crustal section was exhumed.

3.4. Significance of Lower Crustal Rocks in the Flanks of Slow Spreading Ridges and Implications for Ridge Flank Geochemical Budgets

Outcrops of serpentinized peridotites and hydrothermally altered gabbros have been reported from many locations along the slow spreading Mid-Atlantic Ridge (MAR), Cayman Trough, and the ultraslow spreading Southwest Indian Ridge (SWIR) (Bonatti and Honnorez, 1976; Cannat et al., 1992, 1995; Dick, 1989; Engeln and Fisher, 1969, 1975; Ito and Clayton, 1983; Mével, 1987, 1988; Mével et al., 1991; Meyer et al., 1989). These exposures of plutonic and ultramafic rocks are not restricted to transform fault walls (Aumento and Loubat, 1971). Gabbroic rocks and peridotites have been recovered in abundance from rift valley walls and from uplifted basement blocks within inside-corner tectonic settings near the ends of

Table 4. Changes of element concentration per percent alteration in different alteration zones of Hole 735B.

Zone	1	2+3	4	5+6	1'	2'
Depth range	500–600	600–1050	1050–1300	1300–1500	0–40	40–500
Alteration type	Oxidative	Nonoxid.	Nonoxid.	Nonoxid.	Oxidative	Nonoxid.
Intensity of alteration	Moderate	Low	Moderate	Low	Moderate	Low
SiO ₂	–0.2 (0.1)	–0.1 (0.03)	0 (0.1)	0 (0.1)	–0.2 (0.1)	–0.1 (0.03)
MgO	–0.2 (0.2)	0 (0.1)	–0.2 (0.2)	–0.2 (0.2)	–0.2 (0.2)	0 (0.1)
CaO	–0.2 (0.2)	0 (0.1)	0 (0.1)	0 (0.1)	–0.2 (0.2)	0 (0.1)
Na ₂ O	0 (0.1)	0 (0.03)	0.06 (0.04)	0.04 (0.04)	0 (0.1)	0 (0.03)
CO ₂	0.1 (0.1)	0.02 (0.02)	0.03 (0.03)	0.01 (0)	0.1 (0.1)	0.02 (0.02)
H ₂ O	0.05 (0.05)	0.07 (0.04)	0.1 (0.02)	0.08 (0.04)	0.05 (0.05)	0.07 (0.04)
K ₂ O (× 10 ^{–3})	2 (4)	0 (1)	7 (7)	2 (2)	22 (4) ^a	0 (1)
P ₂ O ₅ (× 10 ^{–3})	4 (3)	0 (2)	0 (1)	0 (1)	18 (7) ^a	0 (2)
S (× 10 ^{–3})	0 (1)	30 (30)	6 (9)	8 (8)	0 (1)	30 (30)
Li (× 10 ^{–4})	0 (0.4)	0.14 (0.04)	0.5 (0.5)	0.2 (0.2)	0 (0.4)	0.14 (0.04)
Rb (× 10 ^{–4})	0.05 (0.05)	0 (0.01)	0.04 (0.03)	0.02 (0.01)	0.4 (0.1) ^a	0 (0.01)
Cs (× 10 ^{–6})	0.3 (0.5)	0 (0.1)	0.1 (0.1)	0.03 (0.03)	2 (0.1) ^a	0 (0.1)
U (× 10 ^{–6})	2 (0.3)	0.03 (0.03)	0.02 (0.02)	0 (0.02)	0.2 (0.04) ^a	0.03 (0.03)

Concentration changes for zones from interval between 500 and 1500 mbsf are calculated from data in Tables 1 and 2. The total change in concentration of an element $\Delta C = (C - M_f/M_a * C_a)/(M_f/M_a)$, where $M_f/M_a = [TiO_2]_f/[TiO_2]_a$ (Grant, 1986) is divided by the difference in degree of alteration between fresh and altered rock to derive the concentration change in g/100g per percent alteration. Numbers in brackets give approximate uncertainty in the estimate based on scatter in the data.

For the uppermost 500 mbsf, a rough estimate of concentration change per percent alteration has been made based on the assumption that these changes are comparable to the ones determined in this study for zones from below 500 mbsf with similar alteration styles and intensities.

^a Concentration changes for K₂O, P₂O₅, Rb, Cs, and U have been estimated on the basis of the average concentrations of these elements in the shallowest three strip samples examined by Hart et al. (1999). These data suggest that the uppermost 40 meters have gained 0.12 (±0.02) wt.% K₂O, 0.09 (±0.05) wt.% P₂O₅, 0.1 (±0.03) ppm Cs, 1.8 (±0.4) ppm Rb, and 0.010 (±0.002) ppm U relative to fresh protoliths (Hart et al., 1999). It has been assumed that the degree of low-temperature alteration of the strip samples is 5% (cf. Fig. 4).

spreading segments (Tucholke and Lin, 1994). Most exposures of lower crust and upper mantle lithologies along ridges with low magma budgets are believed to be the result of exhumation along low-angle detachment faults (Dick et al., 1981; Karson,

1990; Tucholke and Lin, 1994; Tucholke et al., 1998). However, recent work has indicated that large detachment faults are not always required to expose mantle rocks at the seafloor in areas of extremely low magma supply (Cannat et al., 1997; Lagabrielle et al., 1998). For example, in the 15°N region at the Mid-Atlantic Ridge, slip seems to be accommodated not by a large detachment fault but by a complex fault system with frequently changing polarity (Cannat et al., 1997).

Estimating how alteration of upper mantle and lower crustal lithologies affects global geochemical budgets requires a better knowledge of the abundance and spatial distribution of plutonic and ultramafic rocks at the sea floor. It seems likely that elemental exchange calculated for alteration of crust generated at magmatically robust spreading ridges is not representative for a large fraction of slow and ultraslow spreading ridge segments. By length, spreading ridges with full rates <40 mm/yr make up 52% of the global mid-ocean ridge system (Baker et al., 1996). This corresponds to roughly 20% of the sea floor produced per year. The fraction of sea floor with lower crustal/upper mantle lithologies along the slow and ultraslow spreading ridges is not known. However, estimates for the MARK area suggest that ~23% of the sea floor is mantle rocks (Cannat et al., 1995); hence, for our calculations we assume a value of 25%. This then implies that only 5% of the new sea floor produced per year (3 km²/yr) consists of outcrops of plutonics and mantle rocks.

Based on this estimate, global geochemical fluxes have been estimated for low-temperature alteration of exposed lower oceanic crust (Table 6). These flux estimates are one or two orders of magnitude lower for most elements than those for other volcanic ridge flanks. The Hole 735B fluxes are also insignificant when compared to continental runoff and axial high-

Table 5. Estimated mass changes for low-grade alteration of basaltic and gabbroic crust.

	Staudigel et al. (1996) 500 m 417/418	Alt et al. (1996) 600 m 504B	This work ^a 1500 m 735B
SiO ₂ (g/100 g)	+1.2	+1.0	+0.1
MgO (g/100 g)	–0.2	+0.3	–0.2
CaO (g/100 g)	+2.1	–0.1	–0.1
Na ₂ O (g/100 g)	+0.15	+0.09	+0.03
K ₂ O (g/100 g)	+0.54	+0.13	+0.01
P ₂ O ₅ (g/100 g)	+0.006	+0.003	+0.003
CO ₂ (g/100 g)	+3.26	+0.12	+0.06
H ₂ O (g/100 g)	+2.81		+0.11
S (g/100 g)		–0.06 ^b	+0.02
Li (mg/kg)		+3.3 ^c	+0.3
Rb (mg/kg)	+9 ^d	+1.1 ^c	+0.07
Cs (mg/kg)	0.14 ^d	+0.03 ^c	+0.003
U (mg/kg)	+0.25 ^d	+0.06 ^c	+0.007

^a Mass change estimates in this study have been made based on the assumption that Ti is immobile. The differences between the concentrations C of elements in altered rocks and those in corresponding fresh rocks have been plotted versus the degree of alteration to derive ΔC per % alteration for the different alteration zones. These numbers have been multiplied with the visually estimated degree of low-grade background alteration to generate synthetic logs for downhole variation in ΔC . Mass changes for elements in the drill hole have been calculated by integrating ΔC over the entire depth interval.

Additional data sources: ^b Alt (1995), ^c Bach (unpublished data), ^d Hart and Staudigel (1982).

Table 6. Various estimates for hydrothermal fluxes in ridge flanks, compared with hydrothermal fluxes at mid-ocean spreading ridges and river fluxes.

		Flank fluxes				Axial fluxes		Dissolved river flux
		Staudigel et al. (1996) 500 m 417/418	Alt et al. (1996) 600 m 504B	Wheat & Mottl (2000) JdFR flank	This work ^a 1500 m 735B	Low	High	
Si	10 ⁹ mol/yr	-700	-740	18	8	100	1100	6400
Mg	10 ⁹ mol/yr	170	-340	-5400	20	-960	-2600	5400
Ca	10 ⁹ mol/yr	-1400	-6	4700	-5	5.4	2200	12000
Na	10 ⁹ mol/yr	-20	-28	-620	-1			5700
K	10 ⁹ mol/yr	-210	-60	-330	-0.3	100	1100	1900
P	10 ⁹ mol/yr		-1.0	-0.3	-0.1	-0.05	-0.12	33
C	10 ⁹ mol/yr	-2700	-120	-160	-6	62	1300	32000
H ₂ O	10 ⁹ mol/yr	-5600		-2100	-27			
S	10 ⁹ mol/yr		77 ^c	-3				103
Li	10 ⁹ mol/yr		-2 ^c		-0.02	-0.7	7	6314
Rb	10 ⁶ mol/yr	-490 ^d	-55 ^c	-26	-0.3	160	1500	370
Cs	10 ⁶ mol/yr	-6.5 ^d	-1 ^c		-0.01	1.8	9.8	4.8
U	10 ⁶ mol/yr	-9.7 ^d	-1 ^c	-1.4	-0.01	-0.23	-0.64	45

^a Crustal production rate is 0.225 km³/yr (3 km² × 0.05 × 1.5 km), based on the assumption that 5% of ocean floor is uplifted gabbro.

Additional data sources: ^b Alt (1995), ^c Bach (unpublished data), ^d Hart and Staudigel (1982). Data source for axial fluxes and dissolved river flux is Mottl et al. (1994).

temperature hydrothermal fluxes. However, for some elements the estimated fluxes are significant. For example, the calculated S flux (3 × 10⁹ mol/yr) is approaching those related to microbial sulfate reduction during low-temperature (<200°C) serpentinization of abyssal peridotites (13–440 × 10⁹ mol/yr; Alt and Shanks, 1998), and corresponds to 3% of the riverine sulfate input and 5% of sedimentary sulfide output. Hence, these data suggest that low-temperature alteration of uplifted lower crust, as well as serpentinization of peridotites, may provide an important sink for S in the marine environment. Moreover, the calculated flux for Mg suggests that low-temperature alteration of lower crust may be a small source of Mg. Snow and Dick (1995) observed Mg losses in serpentinized peridotites weathered at the sea floor and proposed that sea floor weathering of serpentinites may result in a significant flux of Mg to the oceans, probably through dissolution of brucite and breakdown of olivine. Hence, although the Mg fluxes estimated for Hole 735B are insignificant in comparison with the riverine input, fluid circulation in the flanks of slow spread crust may constitute a source of Mg to the oceans.

It should be noted that the role low-temperature alteration of lower crust plays in global fluxes may be more important than suggested by the small fluxes inferred from Hole 735B because ongoing seawater circulation will result in continued exchange between sea water and Atlantis Bank basement. In general, chemical exchange between the oceans and lower crustal/upper mantle rocks may be more important than indicated by the relatively small fraction of sea floor made up of these lithologies. Peridotite and gabbro outcrops are commonly associated with rough basement topographies and bathymetric highs such as uplifted blocks at inside-corner highs and transverse ridges flanking fracture zones. At these locations, exchange between lithosphere and seawater may be sustained for longer periods of time than in normal ridge flanks with smooth topographies, where a veneer of sediments will limit exchange with the oceans.

4. CONCLUSIONS

Low-grade alteration of tectonically exposed lower crust at Hole 735B is not restricted to the immediate subsurface (sea-floor weathering) but extends down to at least 1500 m below the seafloor. Alteration is most pronounced in areas with high vein densities. Chemical data for 18 fresh/altered sample pairs of gabbroic rocks indicate that overall changes related to low-grade alteration are gains in H₂O, CO₂, S, alkalis, U, P, ¹⁸O, and ⁸⁷Sr, and possibly slight losses in Mg, Ca, and Si. Chemical changes calculated for 1.5 km of Hole 735B-like crust indicate that Na, and P increase is similar to those calculated for some volcanic ridge flanks.

CO₂ increase estimated for Hole 735B is similar to that calculated for young (<6 Ma) volcanic ridge flanks and an order of magnitude lower than estimates for old ridge flanks (>110 Ma). The concentrations of CO₂ in Hole 735B are high compared to gabbros from other areas. This difference could be related to the older age (12 Ma) for Hole 735B compared to the other sites (<1 Ma), indicating that uptake of C may be a continuous process in exposed lower oceanic crust.

Chemical changes for other elements are an order of magnitude or more lower than volcanic ridge flank fluxes, reflecting the overall low extent of low-grade alteration (around 2%). Our estimate for S fluxes suggests that uplifted lower oceanic crust provides a small sink for sulfur and a small source for Mg, in contrast to volcanic ridge flanks that appear to act as a S source and Mg sink. Global fluxes related to low-grade alteration of uplifted lower crust are insignificant when compared to riverine input, reflecting both the overall low extent of alteration and the fact that lower crustal rocks probably make up less than 5% of the sea floor.

The rough basement topography of slow and ultraslow spread crust may promote continued basement–seawater interaction, which is largely inhibited by a sediment blanket covering volcanic ridge flanks. In this regard the fluxes calculated based on Hole 735B may represent minimum estimates. More

work is required to better define the significance of reactions between seawater and lower crust/upper mantle in global lithosphere–seawater exchange.

Acknowledgments—This study was made possible through grants from a JOI/USSSP (F000767) and NSF (OCE 9907070). We would like to thank the crew of the JOIDES Resolution and the excellent technical staff provided by the Ocean Drilling Program. WB acknowledges support from J. Lamar Worzel and Penzance Endowed Funds, and YN acknowledges support from the Australian Research Council. Many thanks to Daniel Bideau for providing his visual estimates of low-grade alteration for the 500 to 1500 mbsf interval. We are grateful to Mark Kurz for providing access to the TIMS facility at WHOI and to Jerzy Blusztajn for running the mass spectrometer. Helpful suggestions by Damon Teagle and two anonymous reviewers are greatly appreciated. This is WHOI Contribution 10459.

Associate editor: F. A. Frey

REFERENCES

- Alt J. C. (1995) Sulfur isotope profile through the oceanic crust: Sulfur mobility and seawater–crustal sulfur exchange during hydrothermal alteration. *Geology* **23**, 585–588.
- Alt J. C. and Bach W. (2001) Low grade hydrothermal alteration of uplifted lower oceanic crust, ODP Hole 735B (Leg 176): Mineralogy and isotope geochemistry. *Leg 176 Scientific Result Volume*. Submitted.
- Alt J. C. and Honnorez J. (1984) Alteration of the upper oceanic crust, DSDP site 417: Mineralogy and chemistry. *Contrib. Mineral. Petrol.* **87**, 149–169.
- Alt J. C. and Shanks W. C. (1998) Sulfur in serpentinized oceanic peridotites: Serpentinization processes and microbial sulfate reduction. *J. Geophys. Res.* **103**, 9917–9929.
- Alt J. C. and Teagle D. A. H. (1999) The uptake of carbon during alteration of ocean crust. *Geochim. Cosmochim. Acta* **63**, 1527–1535.
- Alt J. C., Teagle D. A. H., Laverne C., Vanko D., Bach W., Honnorez J., and Becker K. (1996) Ridge flank alteration of upper oceanic crust in the eastern Pacific: A synthesis of results for volcanic rocks of Holes 504B and 896A. In *Proc. ODP, Sci. Results*, Vol. 148 (eds. J. C. Alt, H. Kinoshita, L. B. Stokking, and P. J. Michael), pp. 435–450. Ocean Drilling Program.
- Aumento F. and Loubat H. (1971) The Mid-Atlantic ridge near 45 degrees N; XVI, Serpentinized ultramafic intrusions. *Can. J. Earth Sci.* **8**, 631–663.
- Aumento F. (1971) Uranium content of mid-ocean ridge basalts. *Earth Planet. Sci. Lett.* **11**, 90–94.
- Bach W., Erzinger J., Alt J. C., and Teagle D. A. H. (1996) Chemistry of the lower sheeted dike complex, ODP Hole 504B, Leg 148: The influence of magmatic differentiation and hydrothermal alteration. In *Proc. ODP, Sci. Results*, Vol. 148 (eds. J. C. Alt, H. Kinoshita, L. B. Stokking, and P. J. Michael), pp. 39–55. Ocean Drilling Program.
- Baker E. T., Chen Y. J., and Phipps Morgan J. P. (1996) The relationship between near-axis hydrothermal cooling and the spreading rate of mid-ocean ridges. *Earth Planet. Sci. Lett.* **142**, 137–145.
- Barrett, T.J. (1983) Strontium- and lead-isotope composition of some basalts from Deep Sea Drilling Project Hole 504B, Costa Rica Rift, Legs 69 and 70. In *Init. Repts. DSDP* Vol. 69 (eds. J. R. Cann, M. G. Langseth, J. Honnorez, R. P. Von Herzen, S. M. White, et al.), pp. 643–650. U.S. Govt. Printing Office.
- Berger G., Schott J., and Guy C. (1988) Behavior of Li, Rb, and Cs during basalt glass and olivine dissolution and chlorite, smectite and zeolite precipitation from seawater: Experimental investigations and modelization between 50° and 300°C. *Chem. Geol.* **71**, 297–312.
- Berndt M. and Seyfried W. E. (1986) B, Li, and associated trace element chemistry of alteration minerals, Hole 597B and 597C. In *Init. Repts. DSDP* 92 (eds. M. Leinen, D. K. Rea, et al.), pp. 491–497. U.S. Govt. Printing Office.
- Berner R.A. (1973) Phosphate removal from sea water by adsorption on volcanogenic oxides. *Earth Planet. Sci. Lett.* **18**, 77–86.
- Bonatti E. and Honnorez J. (1976) Sections of the Earth's crust in the Equatorial Atlantic. *J. Geophys. Res.* **81**, 4087–4103.
- Campbell A. C., Palmer M. R., Klinkhammer G. P., Bowers T. S., Edmond J. M., Lawrence J. R., Casey J. F., Thompson G., Humphris S., Rona P., and Karson J. A. (1988) Chemistry of hot springs on the Mid-Atlantic Ridge. *Nature* **335**, 514–519.
- Cannat M. (1991) Plastic deformation at an oceanic spreading ridge: A microstructural study of Site 735 gabbros (southwest Indian Ocean). *Proc. ODP. Sci. Results* **118**, 399–408.
- Cannat M. (1996) How thick is the magmatic crust at slow spreading oceanic ridges? *J. Geophys. Res.* **101**, 2847–2857.
- Cannat M., Bideau B., and Bougault H. (1992) Serpentinized peridotites and gabbros in the Mid-Atlantic Ridge axial valley at 15°37'N and 16°52'N. *Earth Planet. Sci. Lett.* **109**, 87–106.
- Cannat M., Lagabrielle Y., de Coutures N., Bougault H., Casey J., Dmitriev L., and Fouquet Y. (1997) Ultramafic and gabbroic exposures at the Mid-Atlantic Ridge: Geological mapping in the 15°N region. *Tectonophysics* **279**, 193–213.
- Cannat M., Mével C., Maia M., Depluis C., Durand C., Gente P., Agrinier P., Belarouchi A., Dubuisson G., Humler E., and Reynolds J. (1995) Thin crust, ultramafic exposures, and rugged faulting patterns at the Mid-Atlantic Ridge (22°–24°N). *Geology* **23**, 49–52.
- Christie D. M., Carmichael I. S. E., and Langmuir C. H. (1986) Oxidation states of mid-ocean ridge basalt glasses. *Earth Planet. Sci. Lett.* **79**, 397–411.
- Corliss J. B., Dymond J., Gordon L. I., Edmond J. M., Von Herzen R. P., Ballard R. D., Green K., Williams D., Bainbridge A., Crane K., and Van Andel T. H. (1979) Submarine thermal springs on the Galapagos Rift. *Science* **203**, 1073–1083.
- de Villiers S. and Nelson B. K. (1999) Detection of low-temperature hydrothermal fluxes by seawater Mg and Ca anomalies. *Science* **285**, 721–723.
- Dick H. J. B. (1989) Abyssal peridotites, very slow spreading ridges and ocean ridge magmatism. In *Magmatism in the Ocean Basins* (eds. A. D. Saunders and M. J. Norry), pp. 71–105. Blackwell.
- Dick H. J. B., Meyer P. S., Bloomer S., Kirby S., Stakes D., and Mawer C. (1991a) Lithostratigraphic evolution of an *in-situ* section of Oceanic Layer 3. In *Proc. ODP. Sci. Results*, Vol. 118 (eds. R. P. Von Herzen, P. T. Robinson, et al.), pp. 439–538. Ocean Drilling Program.
- Dick H. J. B., Natland J. H., Alt J. C., Bach W., Bideau D., Gee J. S., Haggas S., Hertogen J. G. H., Hirth G., Holm P. M., Ildefonse B., Iturrino G. J., John B. E., Kelley D. S., Kikawa E., Kingdon A., LeRoux P. J., Maeda J., Meyer P. S., Miller D. J., Naslund H. R., Niu Y., Robinson P. T., Snow J., Stephen R. A., Trimby P. W., Worm H.-U., and Yoshinobu A. (2000) A long in situ section of the lower ocean crust: Results of ODP Leg 176 Drilling at the Southwest Indian Ridge. *Earth Planet. Sci. Lett.* **179**, 31–51.
- Dick H. J. B., Schouten H., Meyer P. S., Gallo D. G., Bergh H., Tyce R., Patriat P., Johnson K. T. M., Snow J., and Fisher A. (1991b) Tectonic evolution of the Atlantis II Fracture Zone. In *Proc. ODP. Sci. Results*, Vol. 118 (eds. R. P. Von Herzen, P. T. Robinson, et al.), pp. 359–398.
- Dick H. J. B., Thompson G. A., and Bryan W. B. (1981) Low-angle faulting and steady-state emplacement of plutonic rocks at ridge-transform intersections. *EOS* **62**, 406.
- Edmond J. M., Measures C., Mangum B., Grant B., Sclater F. R., Collier R., and Hudson A. (1979) On the formation of metal-rich deposits at Ridge crests. *Earth Planet. Sci. Lett.* **46**, 19–30.
- Elderfield H., Wheat C. G., Mottl M. J., Monnin C., and Spiro B. (1999) Fluid and geochemical transport through oceanic crust: A transect across the eastern flank of the Juan de Fuca Ridge. *Earth Planet. Sci. Lett.* **172**, 151–165.
- Elthon D., Lawrence J. R., Hanson R. E., and Stern C. (1984) Modeling of oxygen-isotope data from the Sarmiento ophiolite complex, Chile. In *Ophiolites and Oceanic Lithosphere* (eds. I. G. Gass, S. J. Lippard, and A. W. Shelton), pp. 185–197. Blackwell Scientific Publishers.
- Engeln C. G. and Fisher R. L. (1969) Lherzolite, anortosite, gabbro, and basalt dredged from the Mid-Atlantic Ridge. *Science* **166**, 1136–1141.
- Engeln C. G. and Fisher R. L. (1975) Granitic to ultramafic rock

- complexes of the Indian Ocean ridge system, western Indian Ocean. *Geol. Soc. Am. Bull.* **86**, 1553–1578.
- Fletcher J. M., Stephens C. J., Petersen E. U., and Skerl L. (1997) Greenschist facies hydrothermal alteration of oceanic gabbros: A case study of element mobility and reaction paths. In *Proc. ODP Sci. Results 153* (eds. J. A. Karson, M. Cannat, D. J. Miller, and D. Elthon), pp. 389–398. Ocean Drilling Program.
- Grant, J.A. (1986) The isocon diagram—a simple solution to Gresens's equation for metasomatic alteration. *Econ. Geol.* **81**, 1976–1982.
- Gregory R. T. and Taylor H. P. (1981) An oxygen isotope profile in a section of Cretaceous oceanic crust, Samail ophiolite, Oman: Evidence for $d^{18}O$ buffering of the oceans by deep (>5km) seawater-hydrothermal circulation at mid-ocean ridges. *J. Geophys. Res.* **86**, 2737–2755.
- Hart S. R., Blusztajn J., Dick H. J. B., Meyer P. S., and Muehlenbach K. (1999) The fingerprint of seawater circulation in a 500-meter section of ocean crust gabbros. *Geochim. Cosmochim. Acta* **63**, 4059–4080.
- Hart S. R. and Staudigel H. (1982) The control of alkalis and uranium in seawater by ocean crust alteration. *Earth Planet. Sci. Lett.* **58**, 202–212.
- Hart S. R. and Staudigel H. (1986) Ocean crust vein mineral deposition: Rb/Sr ages, U-Th-Pb geochemistry, and duration of circulation at DSDP sites 261, 462 and 516. *Geochim. Cosmochim. Acta* **50**, 2751–2761.
- Haymon R. M. and Kastner M. (1981) Hot spring deposits on the East Pacific Rise at 21°N: Preliminary description of mineralogy and genesis. *Earth Planet. Sci. Lett.* **53**, 363–381.
- Ito E. and Clayton R. N. (1983) Submarine metamorphism of gabbros from the Mid-Cayman Rise: An oxygen isotopic study. *Geochim. Cosmochim. Acta* **47**, 535–546.
- Ito E., White W. M., and Göpel C. (1987) The O, Sr, Nd and Pb isotope geochemistry of MORB. *Chem. Geol.* **62**, 157–176.
- Jannasch H. W. and Mottl M. J. (1985) Geomicrobiology of deep-sea hydrothermal vents. *Science* **229**, 717–725.
- John B. E., Foster D. A., Murphy J. M., Fanning C. M., and Copeland P. (2001). Quantitative age and thermal history of in-situ lower oceanic crust - Atlantis Bank, Southwest Indian Ridge. *Earth Planet. Sci. Lett.* Submitted.
- Karson J. A. (1990) Seafloor spreading on the Mid-Atlantic Ridge: Implications for the structure of ophiolites and oceanic lithosphere produced in slow-spreading environments. In *Ophiolites, Oceanic Crustal Analogues, Proceedings of the Symposium "Troodos 1987"* (eds. J. Malpas, E. Moores, A. Panayiotou, and C. Xenophontos), pp. 547–555. The Geological Survey Department Ministry of Agriculture and Natural Resources.
- Kawahata H., Kusakabe M., and Kikuchi Y. (1987) Strontium, oxygen and hydrogen isotope geochemistry of hydrothermally altered and weathered rocks in DSDP Hole 504B, Costa Rica Rift. *Earth Planet. Sci. Lett.* **85**, 343–355.
- Kelley D. S. (1996) Methane-rich fluids in the oceanic crust. *J. Geophys. Res.* **101**, 2943–2962.
- Kelley D. S. and Früh-Green G. L. (1999) Abiogenic methane in deep-seated mid-ocean ridge environments: Insights from stable isotope analyses. *J. Geophys. Res.* **104**, 10439–10460.
- Kempton P. D., Hawkesworth C. J., and Fowler M. (1991) Geochemistry and isotopic composition of Gabbros from Layer 3 of the Indian Ocean crust, Hole 735B. In *Proc. ODP Sci. Results*, Vol. 118 (eds. R. P. Von Herzen, P. T. Robinson, et al.), pp. 127–143. Ocean Drilling Program.
- Koski R. A., Clague D. A., and Oudin E. (1984) Mineralogy and chemistry of massive sulfide deposits from the Juan de Fuca Ridge. *Geol. Soc. Am. Bull.* **95**, 930–945.
- Kwocien W. (1990) *Silicate Rock Analysis by ICP-AES*. School of Geology, Queensland University of Technology, Australia.
- Lagabrielle Y., Bideau D., Cannat M., Karson J. A., and Mével C. (1998) Ultramafic-mafic rock suites exposed along the Mid-Atlantic Ridge (10°N–30°N). Symmetrical-asymmetrical distribution and implications for seafloor spreading processes. In *Faulting and Magmatism at Mid-ocean Ridges*, Geophysical Monograph Vol. 106 (eds. W. R. Buck, P. T. Delaney, J. A. Karson, and Y. Lagabrielle), pp. 153–176. American Geophysical Union.
- Mével C. (1987) Evolution of oceanic gabbros from DSDP Leg 82: Influence of the fluid phase on metamorphic crystallizations. *Earth Planet. Sci. Lett.* **83**, 67–79.
- Mével C. (1988) Metamorphism in oceanic layer 3, Gorringer Bank, Eastern Atlantic. *Contrib. Mineral. Petrol.* **100**, 496–509.
- Mével C., Cannat M., Gente P., Marion E., Auzende J. M., and Karson J. A. (1991) Emplacement of deep crustal and mantle rocks on the west median valley wall of the MARK area (MAR, 23° N). *Tectonophysics* **190**, 31–53.
- Meyer P. S., Dick H. B., and Thompson G. (1989) Cumulate gabbros from the Southwest Indian Ridge, 54°S–7°16' E: Implications for magmatic processes at a slow spreading ridge. *Contrib. Mineral. Petrol.* **103**, 44–63.
- Mitchell W. S. and Aumento F. (1977) The distribution of uranium in oceanic rocks from the Mid-Atlantic Ridge at 36°N. In *Init. Repts. DSDP 37* (eds. F. Aumento and W. G. Melson), pp. 547–559. U.S. Govt. Printing Office.
- Mottl M. J. and Wheat C. G. (1994) Hydrothermal circulation through mid-ocean ridge flanks: Fluxes of heat and magnesium. *Geochim. Cosmochim. Acta* **58**, 2225–2237.
- Mottl M., Dixon J., Alt J., Humphris S., Lilley M., Rona P., and Sansone F. (1994) Hydrothermal flux working group summary. In *RIDGE/VENT Workshop Report* (eds. D. Kadko, E. Baker, J. Alt, and J. Barross), pp. 4–15. RIDGE office.
- Muehlenbach K. and Clayton R.N. (1972a) Oxygen isotope studies of fresh and weathered submarine basalts. *Can. J. Earth Sci.* **9**, 172–184.
- Muehlenbach K. and Clayton R.N. (1972b) Oxygen isotope studies of submarine greenstones. *Can. J. Earth Sci.* **9**, 471–478.
- Niu Y. and Batiza R. (1997) Trace element evidence from seamounts for recycled oceanic crust in the Eastern Pacific mantle. *Earth Planet. Sci. Lett.* **148**, 471–483.
- Porter S., Vanko D. A., and Ghazi A. M. (2000). Major and trace element compositions of secondary clays in basalts altered at low temperature, eastern flank of the Juan de Fuca Ridge. *Proc. ODP, Sci. Results*, 168 (eds. A. T. Fisher, E. E. Davis, and C. Escutia) [Online]. Available from World Wide Web: <http://www-odp.tamu.edu/publications/168_SR/VOLUME/CHAPTERS/SR168_12.PDF>. [Cited 2001–03–12].
- Richardson S. H., Hart S. R., and Staudigel H. (1980) Vein mineral ages of old oceanic crust. *J. Geophys. Res.* **85**, 7195–7200.
- Rihs S., Condomines M., and Sigmarsson O. (2000) U, Ra and Ba incorporation during precipitation of hydrothermal carbonates: Implications for 226Ra-Ba dating of impure travertines. *Geochim. Cosmochim. Acta* **64**, 661–671.
- Sansone F. J., Mottl M. J., Olson E. J., Wheat C. G., and Lilley M. D. (1998) CO₂-depleted fluids from mid-ocean ridge-flank hydrothermal springs. *Geochim. Cosmochim. Acta* **62**, 2247–2252.
- Shipboard Scientific Party. (1993) Site 894. In *Proc. ODP Init. Repts.*, 147 (eds. K. Gillis, C. Mével, J. Allan, et al.), pp. 45–108. Ocean Drilling Program.
- Shipboard Scientific Party. (1995) Site 923. In *Proc. ODP Init. Repts.*, 153 (eds. M. Cannat, J. A. Karson, D. J. Miller, et al.). Ocean Drilling Program.
- Shipboard Scientific Party. (1999) Site 735B. In *Proc. ODP, Init. Repts.*, 176 (eds. H. J. B. Dick, J. H. Natland, D. J. Miller, et al.), pp. 1–314. [CD-ROM]. Available from: Ocean Drilling Program, Texas A&M University, College Station, TX 77845–9547.
- Snow J. E. and Dick H. J. B. (1995) Pervasive magnesium loss by marine weathering of peridotite. *Geochim. Cosmochim. Acta* **59**, 4219–4235.
- Stakes D. and Vanko D. A. (1986) Multistage hydrothermal alteration of gabbroic rocks from the failed Mathematician Ridge. *Earth Planet. Sci. Lett.* **79**, 75–92.
- Stakes D., Mével C., Cannat M., and Chaput T. (1991) Metamorphic stratigraphy of Hole 735B. In *Proc. ODP Sci. Results*, Vol. 118 (eds. R. P. Von Herzen and P. T. Robinson), pp. 153–180. Ocean Drilling Program.
- Staudigel H., Hart S. R., and Richardson S. H. (1981) Alteration of the oceanic crust: Processes and timing. *Earth Planet. Sci. Lett.* **52**, 311–327.
- Staudigel H., Hart S. R., Schmincke H.-U., and Smith B. M. (1989) Cretaceous ocean crust at DSDP Sites 417 and 418: Carbon uptake

- from weathering versus loss by magmatic outgassing. *Geochim. Cosmochim. Acta* **53**, 3091–3094.
- Staudigel H., Plank T., While B., and Schmincke H.-U. (1996) Geochemical fluxes during seafloor alteration of the basaltic upper oceanic crust: DSDP Sites 417 and 418. In *Subduction Top to Bottom*, Geophysical Monograph Vol. 96 (eds. G. E. Bebout, D. W. Scholl, S. H. Kirby, and J. P. Platt), pp. 19–38. American Geophysical Union.
- Stein C. A., Stein S., and Pelayo A. (1995) Heat flow and hydrothermal circulation. In *Seafloor Hydrothermal Processes*, Geophysical Monograph Vol. 91 (eds. S. E. Humphris, R. A. Zierenberg, L. S. Mullineaux, and R. E. Thomson), pp. 425–445. American Geophysical Union.
- Teagle D. A. H., Alt J. C., Bach W., Halliday A., and Erzinger J. (1996) Alteration of the upper ocean crust in a ridge flank hydrothermal up-flow zone: Mineral, chemical, and isotopic constraints from ODP Hole 896A. In *Proc. ODP, Sci. Results*, Vol. 148 (eds. J. C. Alt, H. Kinoshita, L. B. Stokking, and P. J. Michael), pp. 119–150. Ocean Drilling Program.
- Teagle D. A. H., Alt J. C., and Halliday A. N. (1998) Tracing the evolution of hydrothermal fluids in the upper oceanic crust: Sr-isotopic constraints from DSDP/ODP Holes 504B and 896A. In *Modern Ocean Floor Processes and the Geological Record*, Geol. Soc. Spec. Publ. Vol. 148 (eds. R.A. Mills and K. Harrison), pp. 81–97, The Geological Society.
- Thompson G. (1973) A geochemical study of the low-temperature interaction of sea-water and oceanic igneous rocks. *EOS Transactions* **54**, 1015–1018.
- Thompson G. (1983) Basalt–seawater interaction. In *Hydrothermal Processes at Seafloor Spreading Centers* (eds. P. A. Rona, K. Bostrom, and K. L. Smith), pp. 225–278. Plenum.
- Tivey M. K. (1995) Modeling chimney growth and associated fluid flow at seafloor hydrothermal vent sites. In *Seafloor Hydrothermal Systems*, Geophysical Monograph Vol. 91 (eds. S. E. Humphris, R. A. Zierenberg, L. S. Mullineaux, and R. E. Thomson), pp. 158–177. American Geophysical Union.
- Tucholke B. E. and Lin J. (1994) A geological model for the structure of ridge segments in slow spreading ocean crust. *J. Geophys. Res.* **99**, 11937–11958.
- Tucholke B. E., Lin J., and Kleinrock M. C. (1998) Megamions and mullion structure defining oceanic metamorphic core complexes on the Mid-Atlantic Ridge. *J. Geophys. Res.* **103**, 9857–9866.
- Vanko D. A. and Stakes D. S. (1991) Fluids in oceanic layer 3: Evidence from veined rocks, Hole 735B, Southwest Indian Ridge. In *Proc. ODP Sci. Results*, Vol. 118 (eds. R. P. Von Herzen and P. T. Robinson), pp. 181–215. Ocean Drilling Program.
- Von Damm K. L., Edmond J. M., Grant B., Measures C., Walden B., and Weiss R. F. (1985) Chemistry of hydrothermal solutions at 21°N, East Pacific Rise. *Geochim. Cosmochim. Acta* **49**, 1031–1053.
- Von Herzen R., Robinson P.T., et al. (1989) *Proc. ODP Init. Reports* **118**, Ocean Drilling Program.
- Wheat C. G. and Mottl M. J. (2000). Composition of pore and spring waters from baby bare: Global implications of geochemical fluxes from a ridge flank hydrothermal system. *Geochim. Cosmochim. Acta* **64**, 629–642.